

THE ORIGIN OF CARBON-ATMOSPHERE WHITE DWARFS
WITH IMPLICATIONS FOR TYPE IA SUPERNOVAE

Bart Hayden Dunlap

A dissertation submitted to the faculty of the University of North Carolina at Chapel Hill
in partial fulfillment of the requirements for the degree of Doctor of Philosophy
in the Department of Physics and Astronomy.

Chapel Hill
2015

Approved by:

J. Christopher Clemens

Charles R. Evans

Christian Iliadis

Daniel E. Reichart

Kurtis A. Williams

© 2015
Bart Hayden Dunlap
ALL RIGHTS RESERVED

ABSTRACT

Bart Hayden Dunlap: The Origin of Carbon-Atmosphere White Dwarfs
with Implications for Type Ia Supernovae
(Under the Direction of J. Christopher Clemens)

This study weaves together two strands that at first do not seem to be intertwined. Type Ia supernovae are the class of explosions crucial to measuring out distances on cosmological scales. In the classical theory of their origin, a white dwarf amasses enough material from a main sequence or giant companion star that its interior carbon ignites and explodes. However, these kinds of binary systems may be too sparse to account for the observed rate of type Ia supernova explosions, and much recent work has gone into exploring alternatives, especially the merger of two white dwarfs (the double degenerate scenario). In merger simulations this either results in a type Ia supernova or, depending on initial conditions, produces a massive white dwarf with a magnetic field.

In this context the discovery of a new class of variable white dwarf stars in our solar neighborhood would not seem relevant, but it is. We present the discovery of the 2nd, 3rd, and 4th variables among the white dwarfs with carbon-dominated atmospheres (the hot DQs), which establishes them as a *class* of variables. We show that the properties of this class are consistent with their being massive white dwarfs that are rotating rapidly with magnetic spots that account for the variability.

Furthermore, we show that the existence of these stars at their observed temperatures represents a conundrum. They have the space motions of an older stellar population but the

temperatures and masses of a younger one. This is best explained if they are the reheated remnants of a binary white dwarf merger. This double degenerate scenario for the origin of the hot DQs neatly explains *all the other curious features of the class*, namely their odd carbon-dominated atmospheres, their magnetic fields, their high masses, and their variability. As white dwarf merger products that did not explode, the hot DQs are “failed” type Ia supernovae. Their properties thus become the best observational endpoints against which to calibrate simulations of type Ia supernovae in the double degenerate scenario, and their formation rate becomes an important piece in computing the fraction of double degenerate binaries that remain as candidates for explosion as type Ia supernovae.

ACKNOWLEDGEMENTS

It seems unlikely to be a mere failure of imagination that I find it hard to envision a better, more enjoyable person to be my advisor than Chris Clemens. He has cultivated my scientific intuition and honed my thinking, and he has been a source of encouragement in science and in life. I am deeply grateful to get to work and think with him.

Aside from Chris, the person I've worked with the most is Brad Barlow, without whom becoming an astronomer would have been far less enjoyable. Whether it's batting around crazy ideas, digging into details, or spending a sleep-deprived week on Cerro Pachon, doing science with Brad is always rewarding. Much that is in these pages was done with him.

Happily we are not yet to the point where our data arrive on our computers seemingly disconnected from the sky we look at and the instruments we use. I've had the good fortune of observing many nights with the SOAR telescope and occasionally getting to stick my head in the Goodman spectrograph. It takes a lot to make an observatory like SOAR work. I'm thankful to those who, decades ago, began working to make it happen, to the many folks who daily, and nightly, keep it going, and to Chris for making one of the best spectrographs in the world and for teaching me its inner workings. I'm also grateful to other members of the Goodman Lab—Ricky O'Steen, Josh Fuchs, and Erik Dennihy—for being good companions during many nights of observing, daily work, and numerous discussions about science.

Moving beyond UNC, I'm grateful that I've gotten to know Darragh O'Donoghue, who makes summers in Chapel Hill more enjoyable and who has let me play along in making

new things. I have also had the pleasure on several occasions to learn from Don Winget and Mike Montgomery, who have been welcoming and hospitable at UT and abroad.

Sometimes an idea needs a little reassurance to get off the ground. I'm grateful to Marten van Kerkwijk for helpful discussions at the first Fifty One Erg conference, which encouraged me that the idea that hot DQs are merger products wasn't crazy. And I'm indebted to Kurtis Williams, who, starting at the white dwarf workshop in Tübingen, has taught me a lot about white dwarfs and hot DQs in particular. I'm glad, also, to have gotten to work with Patrick Dufour and Hugh Harris whose model atmospheres and astrometry have strengthened this work.

My time in Chapel Hill has brought me into contact with many wonderful friends. I am thankful to Andy and Charity Pennock and Steve and Jeannie Cox for showing me true hospitality and much more; to many people at Grace Community Church for being a loving family; to Hank Tarlton and the Brookses for being welcoming and supportive; to Nathan Hudson, Matthew Gillikin, Ben Sammons, James Wolfe, John Houser, and Eliot Meyer for being encouraging roommates and friends; to Nick Williams, Kevin Garrett, Jon McDonald, Harrison Holbrook, Keith Pulling, Logan Groves, Jared Shank, Brent McKnight, Wilson Greene, Pryce Ancona, and Jay Putnam for being good companions around campus, in the library, and in life; to David Smith, Chad Mosby, Jordan Maroon, and Dmitriy Chukhin for being faithful friends and occasional breakfast companions; and to Nathan, Brad, John, Adam, Briana, and Samantha, who made the first and many years of graduate school a good, humane, and often tasty experience.

Peering back to the days before graduate school, I am thankful to the physics and astronomy faculty at the University of Central Arkansas for teaching me physics and introducing me to

astronomical research; to Doug Corbitt, a professor, mentor, and friend for being a source of encouragement and persistent intellectual delight; to Ryan, for friendship, wise counsel, and frivolity; and to Michael Cantrell, for perennial friendship and engaging conversations since childhood.

Much gratitude goes to my parents, Charles and Sandra, for their love and support throughout my life and to my family and community in central Arkansas for providing a wonderful place to grow up. It is also there that I found a remarkable group of high school friends who cultivated my interests in philosophy, science, education, and much else and were a general source of intellectual vitality.

To Jacqueline, my wife, who shows me love, graces my life with beauty, and walks beside me with friendship, I am grateful beyond measure. Without her encouragement, patience, and wisdom, much would be undone.

Finally, thanks be to the prodigal Creator for gracing us with myriad wonders and letting us enjoy the pleasure of finding things out.

TABLE OF CONTENTS

LIST OF TABLES	xi
LIST OF FIGURES	xii
LIST OF ABBREVIATIONS	xiii
1 INTRODUCTION	1
1.1 The Small Things	1
1.1.1 The DQ White Dwarfs	4
1.1.2 Esse Quam Videri: The Hot DQs	6
1.2 The Big Things	9
1.3 The Plan of This Work	10
2 ESTABLISHING A NEW CLASS OF VARIABLE STARS	12
2.1 Experiments with Stars	12
2.2 The Hot DQ Variable Stars	13
2.3 Finding New DQVs	17
2.3.1 Observations of SDSS J2200–0741 and SDSS J2348–0942	18
2.3.2 Pulse Shapes of SDSS J2200–0741 and SDSS J2348–0942	24
2.3.3 Observations of SDSS J1337–0026	26
2.3.4 Another Odd Pulse Shape in SDSS J1337–0026	30
2.3.5 Pulse Shape Summary	32
2.4 Other Relevant DQ Observations	34

2.4.1	The DQ NOVs	34
2.4.2	A Long-Period Hot DQ Variable	35
2.4.3	A Warm DQ Variable	36
2.4.4	Observational Summary	37
2.5	Why Do the Hot DQs Vary?	39
2.5.1	Pulsation vs. Rotation	39
2.6	Where the Photometry Leaves Us	43
3	HOT DQ KINEMATICS	45
3.1	Mergers and Massive White Dwarfs	45
3.1.1	The Mass Distribution of White Dwarf Stars	46
3.1.2	Hot DQ Masses	48
3.1.3	Massive Hot White Dwarfs are Young	48
3.2	Population Kinematics	50
3.3	What the Motions of the Hot DQs Reveal	51
3.3.1	Hot DQs as Double Degenerate Merger Remnants	59
4	STELLAR ARITHMETIC	63
4.1	Cardinality as an Important Physical Property	63
4.2	The Single Degenerate Scenario	65
4.3	The Double Degenerate Scenario	69
4.3.1	The Double Degenerate Merger Rate	70
4.4	How Many Hot DQs Are There?	71
4.4.1	The Hot DQ Formation Rate	73
4.5	Where Do The Hot DQs Go?	75

4.6	Future Research Directions and Further Implications	78
4.6.1	Planets	78
4.6.2	Galactic Merger History	79
4.6.3	Theory	79
4.7	Summary and Conclusion	80
	REFERENCES	88

LIST OF TABLES

2.1	Observations of SDSS J2200–0741 & SDSS J2348–0942	19
2.2	Least-squares fits to SDSS J2200–0741 & SDSS J2348–0942	24
2.3	Observations of SDSS J1337–0026	26
2.4	Least-squares fits to SDSS J1337–0026	30
2.5	Amplitude and phase fits of SDSS J1337–0026	32
2.6	The hot DQ NOVs	35
3.1	Parallaxes, masses, &c. for SDSS J2200–0741 & SDSS J0005–1002	49

LIST OF FIGURES

1.1	Spectra of DQ white dwarfs	5
1.2	Spectra of hot DQ white dwarfs	7
2.1	Spectra of hot DQs with signs of magnetism	14
2.2	Pulse shape comparison with SDSS J1426+5752	16
2.3	Discovery light curves of SDSS J2200–0741 & SDSS J2348–0942	21
2.4	Amplitude spectra of SDSS J2348–0942	22
2.5	Amplitude spectrum of SDSS J2200–0741	23
2.6	Pulse shapes of SDSS J2200–0741 & SDSS J2348–0942	25
2.7	Light curves and amplitude spectra of SDSS J1337–0026	27
2.8	Folded light curves of SDSS J1337–0026	33
2.9	Amplitude spectrum of SDSS J0005–1002	36
2.10	Graphical summary of hot DQ magnetism and variability	38
2.11	Pulse shape of V471 Tau & SDSS J2200–0741	41
3.1	White dwarf mass distribution with hot DQ masses	47
3.2	Kinematic heating and white dwarf cooling	51
3.3	Transverse velocities of SDSS WDs grouped by mass	52
3.4	The extreme kinematics of SDSS J1153+0056	54
3.5	Hot DQ cumulative velocity distribution	56
3.6	Hot DQ UV velocities	58

LIST OF ABBREVIATIONS

AGB	asymptotic giant branch
DA	spectral class of white dwarfs with observed H absorption
DB	spectral class of white dwarfs with observed He absorption
DQ	spectral class of white dwarfs with observed C absorption
DR	data release
MS	main sequence
NOV	not observed to vary
SDSS	Sloan Digital Sky Survey
S/N	signal-to-noise ratio
SN Ia	type Ia supernova
WD	white dwarf

CHAPTER 1: INTRODUCTION

“You know my method. It is founded upon the observation of trifles.”

—Sherlock Holmes

Sometimes a small thing illuminates a large one, like a tiny glowing ember in a dark room. What began as a chase to find and study interesting new white dwarf variables with odd carbon-dominated atmospheres has opened a new chapter in understanding the scale of the cosmos.

1.1 The Small Things

Stars are born through the gravitational collapse of hydrogen-rich gas. After its protons and neutrons are fused together by nuclear processes, gravity completes the project of condensing the assembled matter into a compact, elegant object known as a white dwarf. That the production of such a small thing can sometimes take billions of years, and that the result should prove astrophysically interesting, and indeed useful, in a myriad ways, is a testament that patience sometimes yields unexpected results.

All but roughly 3% of stars will end their lives as white dwarfs.¹ A star of typical mass will fuse hydrogen into helium on the main sequence. Once its supply of hydrogen is depleted, the temperature and density limiting effect of nuclear reactions is removed and the core can shrink and heat up beyond the hydrogen burning limit. After a relatively brief time fusing hydrogen into helium in shells on the red giant branch, the helium core reaches an interior temperature

¹For an excellent general overview of white dwarfs, see Kawaler et al. (1997), which we rely on at various points in this discussion.

that is high enough to begin fusing helium. The helium burning phase on the horizontal branch lasts only a fraction (10% to 20%) of the main sequence lifetime. After its helium is spent, the same process of core contraction ensues while the outer envelope expands and the star becomes redder and more luminous, rising along the asymptotic giant branch (AGB). Here it fuses hydrogen and helium in shells of its envelope. The core, meanwhile, has stopped fusing helium into carbon and oxygen and so has shrunk, yet it is not massive enough to contract further and get hot enough to fuse carbon. At this point, it is supported by degenerate electron pressure and has essentially become the hot white dwarf that will emerge once the envelope completes its cycles of shell fusion and mass loss.

Because they are the outcome of most stars, white dwarf stars bear witness to many things that have gone on in the long history of our Galaxy. For example, because they no longer generate energy, white dwarfs tell us their ages with their temperatures: the hottest ones are young, and the old ones have cooled off (Mestel, 1952). For this reason, a simple count of white dwarfs grouped by brightness—the white dwarf luminosity function—reveals how many stars were being formed at each moment in the past. If the underlying physics governing white dwarf cooling can be well enough constrained, white dwarfs can date the Galaxy's birth (Fontaine et al., 2001; Winget et al., 1987).

Being relatively simple thermodynamic systems that have more or less ceased energy production, one could imagine a Universe in which the cooling of a white dwarf were uneventful and unfailingly predictable. Those we actually observe, however, do some interesting things on their way to the cold temperature of the vacuum. Some of them pulsate, enduring millions of years of star quakes resulting from the oscillating interplay of their thin atmospheres with the radiation trying to escape them (Althaus et al., 2010; Fontaine & Brassard, 2008a; Winget

& Kepler, 2008). Others distill and display debris of disrupted planetary systems allowing us to measure the elemental composition of worlds whose constitution would otherwise be the subject of mere theoretical speculation (Jura & Young, 2014).

Others have stellar companions, which can significantly alter their fate and potentially destroy them. If the companion is a nearby main-sequence star, the white dwarf can gravitationally siphon material from it. This matter, which is predominantly hydrogen, usually settles into a large disk surrounding the star before flowing onto the surface. These systems occasionally announce themselves when they tap into their reserves of potential energy and undergo cataclysmic brightening events (Warner, 2003). In the case of novae, gas accumulates on the surface until its lower layers become sufficiently hot and compact that a thermonuclear runaway involving trace amounts of carbon, nitrogen, and oxygen releases enough energy to explosively remove the accumulated gas from the surface (Starrfield et al., 1972).

If the white dwarf has as its companion another electron degenerate object, and if the two white dwarfs are close enough to interact, the resulting accretion disk is always observed to be helium. Whatever hydrogen the donor had on its surface was transferred early on, and the bulk that remains is entirely helium. The donor stars in these, the AM CVn systems, are presumed to have been formed as He-core white dwarfs when the typical progression of nuclear burning outlined above was truncated as the result of companion-induced mass-loss while it was a red giant star, so the core helium never ignited (Kilic et al., 2014; Solheim, 2010).

Thus we see white dwarfs that accrete hydrogen from main-sequence stars, those that accrete helium from companions that converted most of their hydrogen into helium, and even those that consume rocky material from orbiting planetary fragments. Extrapolating from what we observe into the realm of what might yet await discovery, we at once come to white

dwarfs accreting carbon and oxygen from other carbon/oxygen-core white dwarfs. These should be common: When clumps of hydrogen (the most abundant element in the universe) find themselves in the presence of gravity, the most common result is a carbon/oxygen-core white dwarf, and we see many of these white dwarfs interacting with other objects. Yet, these ubiquitous emanations of stellar evolution have never been caught interacting with one another. The discovery of a variable white dwarf with a carbon-dominated atmosphere by Montgomery et al. (2008) was thus met with some excitement.

1.1.1 The DQ White Dwarfs²

In broad strokes, white dwarfs are usually thought of as falling into the DA and DB spectral classes, i.e., those showing spectral lines of hydrogen and those showing spectral lines of helium. However, the DQs, those with carbon absorption lines, outnumber the DBs in volume-limited counts³ even though there are far more DBs in large, magnitude-limited surveys (Kleinman et al., 2013). This result immediately suggests that a typical DQ is fainter than a typical DB. Indeed, most DQs only appear at relatively cool temperatures, and even though their spectra are dominated by carbon absorption, model atmospheres show that there is typically orders of magnitude more helium than carbon in the atmosphere (Dufour et al., 2005; Koester & Knist, 2006).

That there should be any carbon at all in the atmosphere is curious. Though a huge amount of carbon is present in a white dwarf (the result of He-fusion on the horizontal branch and AGB), its compact nature results in typical surface gravities around 10^8 cm s^{-2} , which leads to

²For a good overview, see Dufour (2011).

³Only 3 DB stars are known within 25 pc of the Sun, a volume currently hosting at least 23 DQs, which are fainter and harder to detect (Sion et al., 2014).

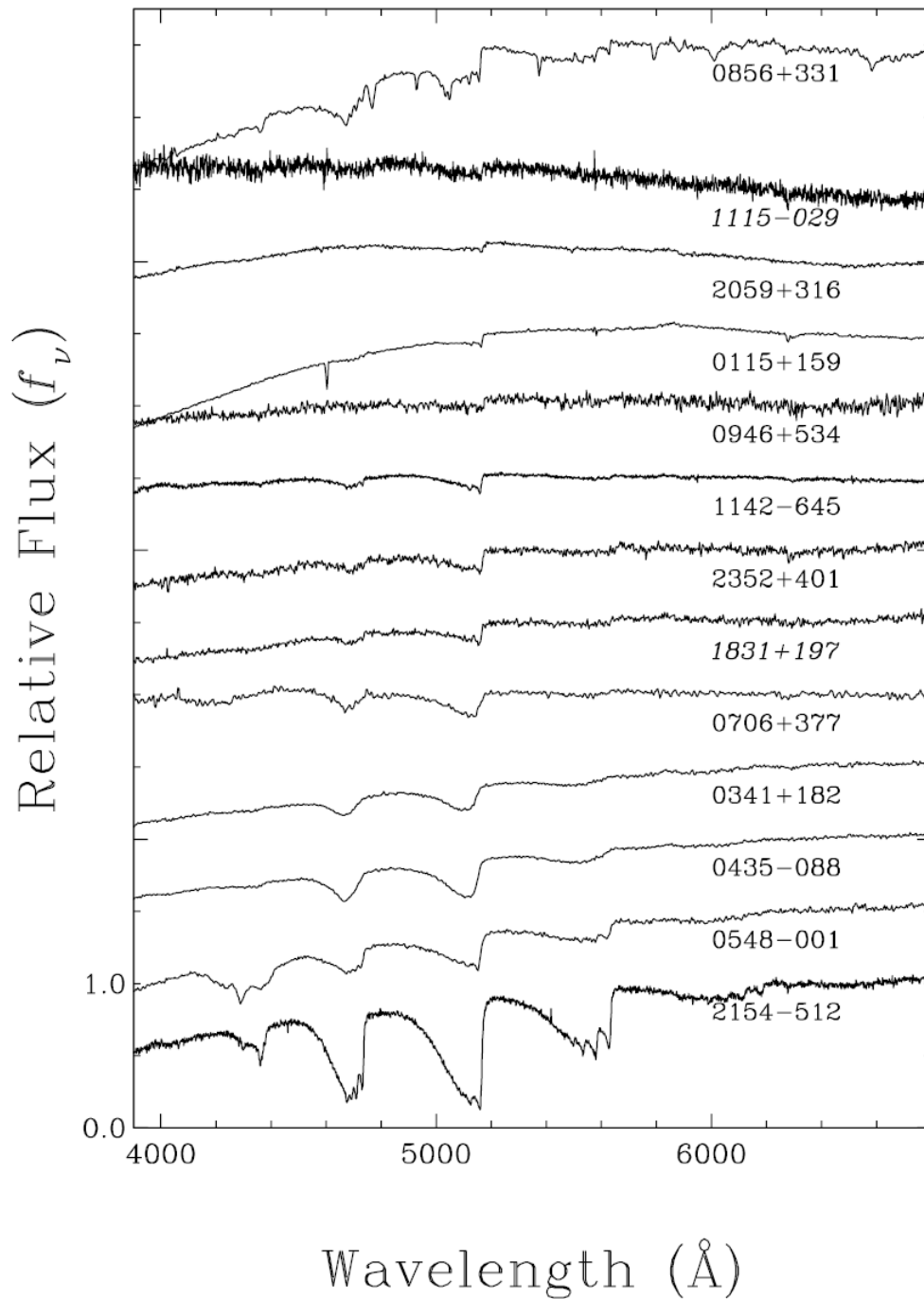


Figure 1.1: The features in these DQ white dwarf spectra are dominated by carbon absorption even though their atmospheres are primarily composed of helium. The spectra at the bottom have atmospheres cool enough to result in broad molecular C_2 Swan bands. The hotter spectra (top) also have absorption lines of neutral $C I$. The temperatures range from $\sim 6,000$ K at the bottom to $\sim 10,000$ K near the top. Figure from Bergeron et al. (2001); reproduced by permission of the AAS.

the atmosphere being stratified by mass.⁴ Thus, any carbon present in the atmosphere should quickly sink and become invisible. The single-element purity of most white dwarf spectra is evidence that this mass segregation happens, yet a white dwarf atmosphere is not a static thing. At certain temperatures, the atmosphere transports energy more efficiently through convection. For helium-atmosphere white dwarfs, the roiling convection zone can extend deep enough to dredge up carbon into the photosphere (Dufour et al., 2005; Koester & Knist, 2006; Pelletier et al., 1986). Because it is only a trace element, it might not be seen at first, but as the star cools, the carbon line opacity increases and the helium absorption decreases resulting in a carbon spectrum (Fig. 1.1) from a helium-dominated atmosphere. Thus the preponderance of carbon-contaminated DQs over DBs at cool temperatures is explained as a natural consequence of spectral evolution (Bergeron et al., 2001).

1.1.2 Esse Quam Videri: The Hot DQs

A few of the DQs, with temperatures from $\sim 25,000$ K to $18,000$ K, form a distinct population. At these temperatures, He I opacities are high and trace amounts of carbon would not be seen. The atmospheric models for these hot DQ white dwarf stars cannot reproduce the observed absorption unless the model atmospheres are actually dominated by carbon (Dufour et al., 2007). Hot DQ spectra (Fig. 1.2) display lines consistent with absorption by ionized carbon (C II), and some also show features corresponding to oxygen lines (Dufour et al., 2010; Liebert et al., 2003). Though the atmospheric models are still being developed, they currently show that some of the hot DQs have as much oxygen as carbon (Dufour et al., 2011b).

The convective dredge-up scenario does not predict that this much core material could be

⁴Such a gravity would increase the speed of an object so quickly that it could traverse the Earth–Moon distance in under 30 s.

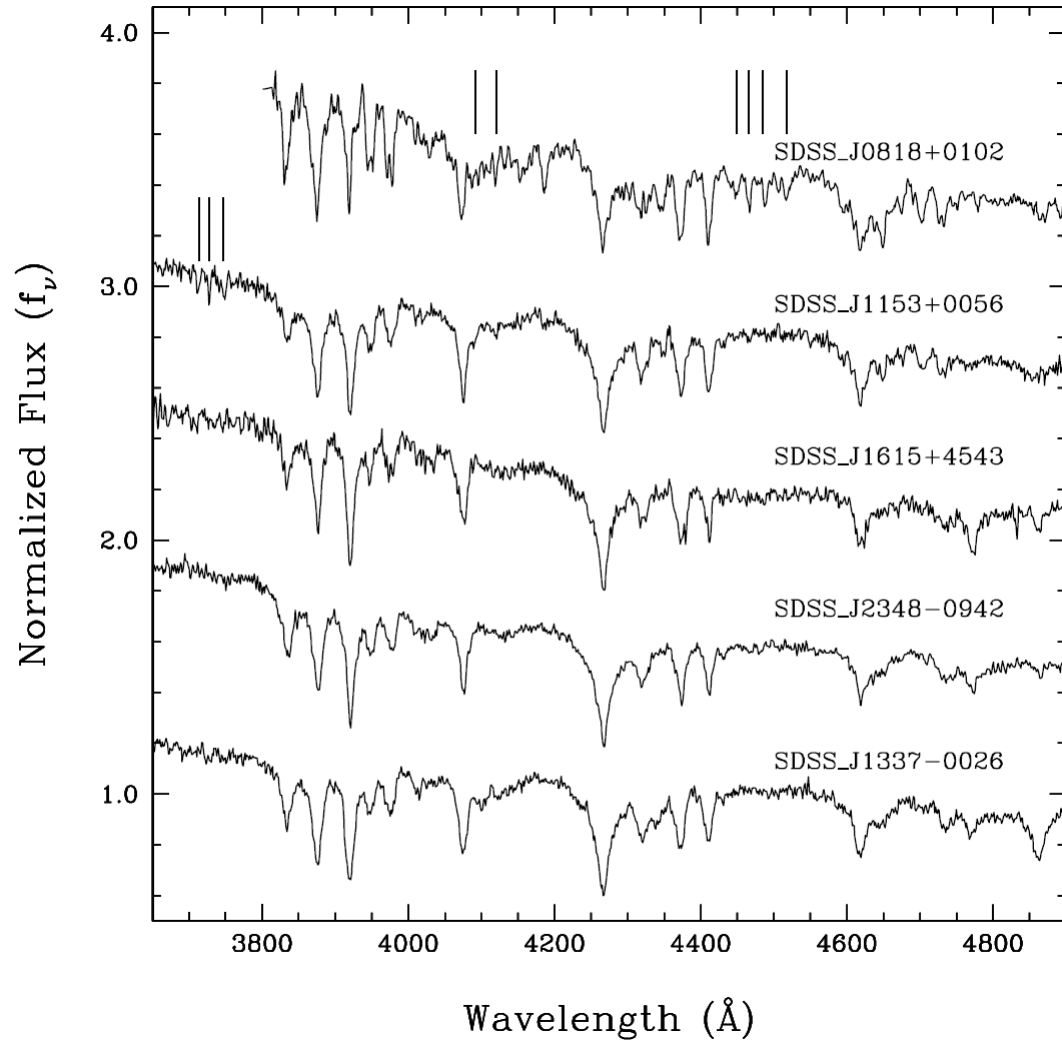


Figure 1.2: Hot DQ spectra are dominated by C II lines and can only be reproduced by atmospheric models with more carbon than helium. Tick marks show absorption by oxygen, which may in some cases be as abundant as carbon. Figure reprinted with permission from Dufour et al. (2010). Copyright 2010, AIP Publishing, LLC.

stirred up into the atmosphere by convection of a typical He layer. This is especially implausible near 20,000 K where the convection zone in the models is relatively shallow (Koester et al., 2014). The discovery of carbon-dominated atmosphere white dwarfs thus presents a challenge. Where does all of this surface carbon (and oxygen) come from?

One proposed scenario is that they are the descendants of stars that had a late He shell flash that burned most of the atmospheric helium (Althaus et al., 2009; Dufour et al., 2008a). This scenario is suggested to explain H1504+65, an extremely hot ($\sim 200,000$ K) star that has just entered the white dwarf cooling track. Its atmosphere consists primarily of carbon and oxygen in equal proportion (Werner et al., 2004). Dufour et al. (2008a) hypothesize that as such a star cools, what little He it retains will float to the top of the atmosphere so that it will have a He spectrum during most of its cooling prior to $\sim 25,000$ K. At that point, the convective motion occurring in the *carbon* layer below will be enough to perturb and mix with the thin He atmosphere above it. The star then would appear as a hot DQ.

Alternatively, the hot DQs might have a binary origin, and thus might result from the expected but so far unobserved interaction of two C/O-core white dwarfs. Seeing the output of such an interaction without ever detecting it in progress suggests it happens quickly. Indeed, theoretical simulations find that carbon mass transfer is unstable, and the binary is expected to rapidly coalesce (Benz et al., 1990). When gravity pulls the two stars together, we would expect the resulting white dwarf star to have an atmosphere over-abundant in carbon and oxygen. However, such a violent merger might also destroy the white dwarfs altogether. Though the two participants were previously unable to fuse carbon in their cores, the merger will result in a massive, hot remnant that may produce the conditions necessary for a thermonuclear runaway, detonating carbon and resulting in a type Ia supernova (Iben & Tutukov, 1984; Webbink,

1984). Thus the hot DQs would be forged by the same process that brings about the most useful calibrators of cosmological distances. That would be useful, because although type Ia supernovae are central to key results of cosmology, their origin is shrouded in darkness.

1.2 The Big Things

Nothing that we know of is quite so large as the universe, and it is getting bigger. Hubble and Lemaître (Hubble, 1929; Lemaître, 1933; Lemaître & MacCallum, 1997) showed that distant galaxies are all moving away from us and that the more distant galaxies are moving away from us more quickly than the closer ones. This is the expectation for an expanding universe,⁵ but characterizing this expansion to know whether it is slowing down, constant, or accelerating requires measuring vast distances precisely. The only tools so far suited to this job rely upon type Ia supernovae, whose explosions are bright enough to be seen in some of the most distant galaxies with measurable velocities (Perlmutter et al., 1999; Riess et al., 1998).

However, seeing a bright explosion in a distant galaxy is not helpful unless we know how much light it is actually giving off. When we know that, a measurement of its apparent brightness can be compared to its intrinsic luminosity to determine its distance. Unfortunately, no two type Ia supernovae have the same intrinsic luminosity. Fortunately, the differences are correlated with other observed properties (Phillips, 1993). Even so, as cosmological investigations become ever-more precise, being able to account more accurately for these intrinsic differences becomes increasingly important. Knowing what causes these explosions would aid this effort, but instead of understanding, there is a good deal of uncertainty (Maoz et al., 2014).

⁵To see this, consider the paradigmatic loaf of raisin bread (the raisins are the galaxies). During the first minute of uniform rising, if all of the raisins move away from each of their neighbors by two morsels, then each moves away from their neighbors' neighbors by four morsels, so the next-door raisins appear to be moving at two morsels per minutes while the more distant ones are receding at a higher rate.

A leading candidate type Ia process is the merging of a double degenerate binary. As double degenerate mergers themselves, the hot DQs would help to sort out the progenitor problem. They would stand as products of the type Ia process that, unlike their exploded siblings, remain intact and so are imprinted with information about the merger that the destroyed remnant has lost,⁶ and they would help us sort out whether there are enough candidate double degenerates to explain the observed Ia rate.

1.3 The Plan of This Work

In what follows we will look at the central question of whether the hot DQs are related to type Ia supernovae or are simply products of a special kind of AGB evolution. We will lay out the observational pieces of the puzzle we have collected and show that it is possible to assemble them into a coherent picture that both makes sense of their peculiar properties and sheds light on uncertain areas of white dwarf evolution and type Ia supernova progenitors. In the next chapter, we will present our discoveries of hot DQ variables and discuss different theories of the origin of their photometric variability. We will argue that the variability arises from the rotation of magnetic features on the surface, making the hot DQs among the most rapidly rotating white dwarfs known. This would be naturally explained if they were spun up in a merger whose swirling plasma also generated a magnetic field.

In chapter 3 we will advance an argument in favor of just such a double degenerate merger origin for the hot DQs. We come to this conclusion because it resolves a conflict between two different ways of measuring white dwarf ages. Calculating their ages from their temperatures and masses, the hot DQs appear to be relatively young members of the Galactic stellar population, which would be consistent with the late helium flash scenario for their origin. However,

⁶Thermonuclear explosions increase entropy by quite a lot.

their space motions, which, like those of all stars, are increasingly perturbed by gravitational encounters over time, are indicative of an older population. This apparent inconsistency is dissolved if the hot DQs have been reheated in a merger event.

In the final chapter we will draw out some implications of this scenario. In particular we will show that the properties of the hot DQs are consistent with their being the expected but apparently missing high mass white dwarfs that result from double white dwarf mergers. Besides demonstrating that such mergers occur, the hot DQs also confirm the theoretical prediction that these events would generate magnetic fields.

Determining the birthrate of this unexploded merger population and subtracting it from the white dwarf merger rate is an essential piece in determining whether there are enough potentially explosive double degenerate mergers to explain a significant fraction of type Ia supernovae. Though the uncertainties are currently large, we will provide a preliminary account that shows broad agreement with the notion that the hot DQs represent a fraction of the expected merged carbon/oxygen double degenerate stars and that the remainder are their close relatives, the type Ia supernovae.

CHAPTER 2: ESTABLISHING A NEW CLASS OF VARIABLE STARS¹

“It is a capital mistake to theorize before one has data. Insensibly one begins to twist facts to suit theories, instead of theories to suit facts.”

—*Sherlock Holmes*

The ancient observational evidence that the heavens were unchanging led Aristotle to a remarkably faulty view of the nature of the heavenly bodies (*On the Heavens*, Book I.3). Interestingly, we can often only make sense of an object when we see it change. This is because the way a thing changes is circumscribed by its nature, and the changes we observe show us the bounds and limits that give an object its identity.

2.1 Experiments with Stars

Much experimental science is about subjecting the objects under study to some sort of change as a way of understanding them better. But stars are far from the poking and prodding of the lab. We cannot heat them in a Bunsen burner, distill their contents in a centrifuge, or mix them together in a beaker to see how they interact. But nature sometimes provides beakers and Bunsen burners of its own, and if we catch them changing—their position, brightness, color, or some combination—we have hope of learning more about them. We have learned that the hot DQs, happily, are not static objects on human timescales, so they offer up more information about themselves and their history than if they were unchanging over centuries.

¹Some content in this chapter previously appeared in *The Astrophysical Journal*. The original citations are as follows: Barlow, B. N., Dunlap, B. H., Rosen, R., & Clemens, J. C. 2008, ApJ, 688, L95, Copyright 2008, The American Astronomical Society and Dunlap, B. H., Barlow, B. N., & Clemens, J. C. 2010, ApJ, 720, L159, Copyright 2010, The American Astronomical Society

There are, of course things we can learn about a star without seeing it change, and here we must keep in mind several important features we glean from (mainly spectroscopic) observations of the static structure of the hot DQs: they all have surface temperatures of roughly 25,000 K to 18,000 K, their atmospheres are dominated by carbon and oxygen, their surface gravities are consistent with a white dwarf mass-radius relationship, and many have magnetic fields (Dufour, 2011). In fact, roughly 70% seem to be magnetic based on high S/N spectroscopic observations (Fig. 2.1); this is much higher than the $\sim 10\%$ incidence of magnetism among white dwarfs in general.

With these properties in mind, we will turn to the exciting discovery of photometric variability in a hot DQ star by Montgomery et al. (2008) and then proceed to present our observations, which resulted in the discovery of three more examples, establishing the hot DQVs as a *class* of variables. We will then discuss the nature of this variability and consider two possible explanations, stellar pulsations and magnetic rotation. We will offer strong reasons for believing the hot DQs are magnetic rotators.

2.2 The Hot DQ Variable Stars

Following the discovery by Dufour et al. (2007) that the atmospheres of the hot DQs and not merely their absorption spectra were dominated by carbon, Montgomery et al. (2008) predicted that these stars might harbor the conditions appropriate for driving stellar pulsations. Both the helium-atmosphere and hydrogen-atmosphere white dwarf stars pulsate in ranges where their dominant atmospheric constituent is partially ionized. The presence of a partial ionization zone has an odd effect on the opacities and heat capacity of a gas. It causes a state where a small compression of the gas allows it to absorb more of the radiation flux passing through on its way to the surface. In this case, when the small, presumably random, compression is relieved,

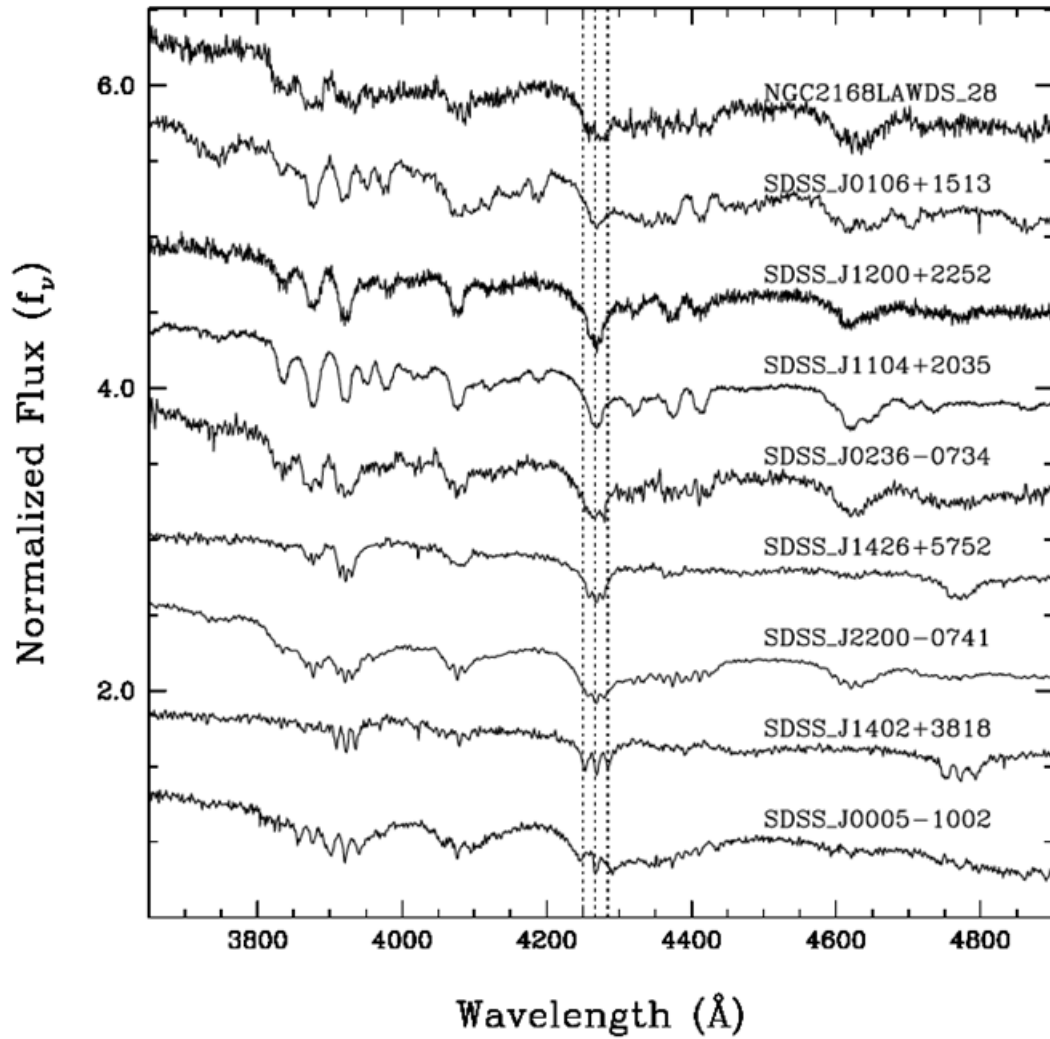


Figure 2.1: A high fraction (70%) of hot DQs display evidence of absorption lines split by magnetic fields. For comparison, the dotted lines running through the figure indicate the expected splitting of the C II $\lambda 4267$ line in the presence of a 2 MG surface field. Cf. the hot DQs in Fig. 1.2, which have smaller or no fields. Figure reprinted with permission from Dufour et al. (2010). Copyright 2010, AIP Publishing, LLC

the gas expands with more vigor than it was compressed. That is, it has the ability to do work on its surroundings, thus transforming the flow of radiative flux into mechanical motions that grow into observable pulsations of the whole star.

Montgomery et al. (2008) calculated the temperature where such pulsations would occur in a carbon-atmosphere white dwarf, found that one star of their six potential hot DQ targets was near this temperature, and then went to the observatory to look at all six. Only one of them was observed to be variable—the one lying closest to the predicted region of pulsation (Degennaro et al., 2008; Montgomery et al., 2008). Perhaps for a moment, the last moment for some time, hot DQ variability seemed to make sense. Yet even though this looked like a rare confirmation of a theoretical prediction, Montgomery et al. (2008) were very cautious in their interpretation of the data, primarily because the shape of the brightness variation does not look like a typical white dwarf pulsator. In Fig. 2.2 we show the comparison from Montgomery et al. (2008) of the pulse shape of the prototype DQV with typical white dwarf pulsators and also an AM CVn system, a white dwarf accreting helium from a white dwarf companion.² Though it does not look like a white dwarf pulsator, the DQs are a crafty bunch; it is hard to know when they are telling the truth and when they are leading us astray. But the more of them we can question, the better chance we have of seeing if their stories line up, so we set out to find more variable DQ stars.

²The possibility of a system currently transferring carbon, analogous to the helium-transferring AM CVn stars, seems to have been ruled out by the absence in hot DQ spectra of high velocity signatures associated with accretion disks (Dufour et al., 2008b).

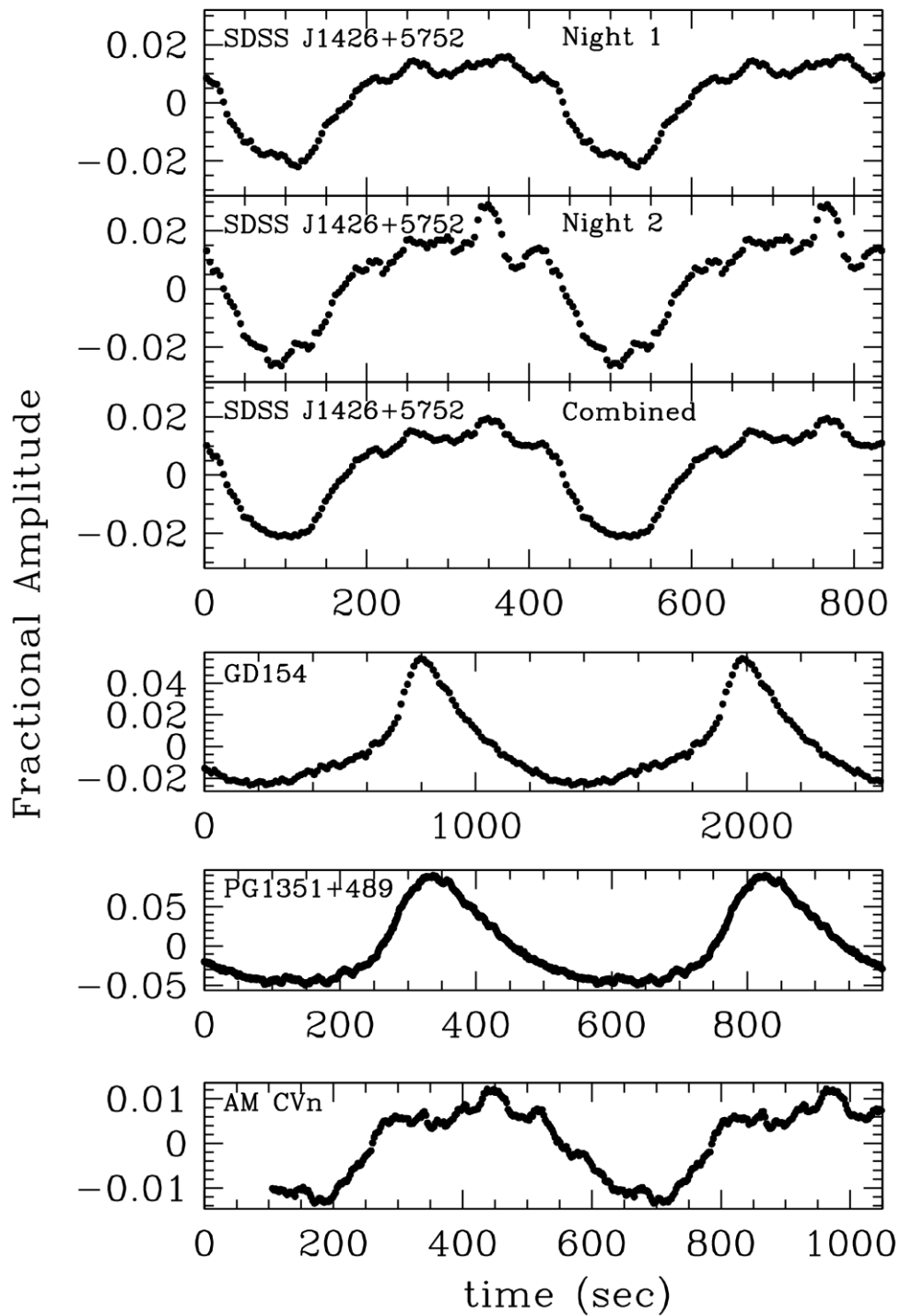


Figure 2.2: The shape of the brightness variation of the prototype variable hot DQ, SDSS J1426+5752 (top three panels) does not look like typical white dwarf pulsators (panels 4, a DA pulsator, and 5, a DB pulsator), which have a family resemblance. Instead, it looks more like the interacting binary white dwarf AM CVn (bottom panel). Figure from Montgomery et al. (2008); reproduced by permission of the AAS.

2.3 Finding New DQVs

Because of the promise of asteroseismology to probe a star's interior,³ the possibility of a new class of pulsating white dwarfs piqued the interest of the white dwarf community, and because of our ready access to telescopes, we were in a favorable position to quickly discover more. We began a photometric survey with the SOAR telescope in Chile, UNC's primary observing facility. Our survey targets came from hot DQs identified (Dufour et al., 2008a) in the Sloan Digital Sky Survey (SDSS). Because the hot DQ stars are relatively rare and faint (median $g = 18.9$), it took a survey the size of the SDSS, which has acquired spectra of thousands of white dwarfs, to unearth them (Liebert et al., 2003). Even though the SDSS is a northern survey, several of the hot DQs are visible from the south. We began observing those available to us and discovered that the first two we looked at were, like SDSS J1426+5752, variable; these two stars had not been observed by Montgomery et al. (2008). We subsequently found variations in SDSS J1337-0026 as well. Because of its very small amplitude ($\sim 0.3\%$), its variability had been below the detection limits of Montgomery et al. (2008) in their survey with the McDonald Observatory 82'' telescope.

These four rapid hot DQ variables have similar properties. Their amplitudes are small, between 0.3% and 1.4%; their periods are relatively short, between 339 s and 1044 s; and they are monophasic. However, only the prototype (SDSS J1426+5752) lies near the region calculated by Montgomery et al. (2008) to have conditions that might readily excite pulsations. Their pulse shapes are either sinusoidal (SDSS J2348-0942) or distorted such that they have

³This is possible because pulsations rattle a star's entire structure, and the way it vibrates depends on many of the fundamental properties (e.g., mass, temperature, elemental composition) of the oscillating material. For the same reason, a brass bell sounds different from a tin one.

deep minima and flat maxima, or even a small secondary dip halfway between minima. We should like to know what gives rise to these phenomena, and we will argue that they are plausibly the result of rotation and magnetism rather than pulsations. Before we advance our case, we will descend into the data since our argument depends, at least in part, on things we have actually observed. The material presented here draws on work published in Barlow et al. (2008) and Dunlap et al. (2010). The cursory reader uninterested in the details might profitably look at the figures and proceed to § 2.3.5 where we briefly discuss the pulse shapes before cataloging some other relevant observations (§ 2.4) and resuming the main story (§ 2.5).

2.3.1 Observations of SDSS J2200–0741 and SDSS J2348–0942

We acquired the bulk of our photometry with the Goodman spectrograph (Clemens et al., 2004) mounted at a Nasmyth port on the 4.1-m SOAR telescope on Cerro Pachon in Chile. On occasions when Goodman was not available, we have also made use of the SOAR Optical Imager (SOI; Schwarz et al. 2004; Walker et al. 2003). To acquire a set of time-series photometry, we took a continuous sequence of exposures to monitor the photometric intensity of an object over time. To minimize dead time between exposures, we often read out only a portion of the available detector, which for Goodman is a $4k \times 4k$ Fairchild 486 back-illuminated CCD. The plate scale at the detector is $0.15 \text{ arcsec pixel}^{-1}$.

We discovered variability in SDSS J2200–0741 and SDSS J2348–0942 on successive nights during an engineering run in June of 2008 and confirmed this a month later. A log of these observations is provided in Table 2.1. Except for the 27 July observation of SDSS J2200–0741, for which there is a five-minute gap in the data, the photometry is uninterrupted. One data set for each object was obtained through a broadband blue S8612 filter; the rest were unfiltered. The CCD readout was unbinned for the 31 July observation of SDSS J2348–0942 but binned

Table 2.1: SDSS J2200–0741 & SDSS J2348–0942 OBSERVATION LOG

Object	UT Date (2008)	Start Time (UTC)	T_{exp} (s)	T_{cycle} (s)	Length (s)	Filter
SDSS J2200–0741	27 Jun	06:57:56	30	34.8	7314	none
	28 Jun	06:00:00	30	34.8	7380	S8612
	27 Jul	02:31:44	25	29.6	6170	none
SDSS J2348–0942	28 Jun	08:47:18	90	95.5	7446	S8612
	31 Jul	05:57:30	55	59.5	9520	none

2×2 for all other data. In order to reduce the cycle time of the exposures, we restricted the readout of the CCD to a subsection of the detector and used an intermediate readout speed (100 kHz). The seeing averages for the runs ranged from $1''$ to $2.5''$, and there was significant moonlight in many of the runs.

We analyzed the data by using a differential photometry program we wrote in IDL that uses the function `APER` (Landsman, 1993), which is based on `DAOPHOT` (Stetson, 1987). We computed signal-to-noise ratio (S/N) estimates with different-sized apertures and used the aperture that maximizes the S/N in the light curve (Howell, 1989). We also performed aperture photometry using the program `CCD_HSP`, an IRAF routine written by Antonio Kanaan. We find that the two photometry programs give comparable results.

Because the amount of time it takes light to travel between a star and our detector varies as our detector is moved around by the Earth, we must correct our observation times to the time the photon would arrive at the solar system’s center of mass. We use the program `WQED` (Thompson & Mullally, 2009) to convert the times from UTC to the barycentric Julian ephemeris date.

The photon flux we measure for our targets is always changing because the Earth’s atmosphere is a source of variable opacity. We correct for this using nearby stars, whose light is traveling through the same patch of atmosphere. Because we only care to measure possible

changes in a star's intrinsic brightness and do not need to measure its brightness in any absolute sense, we divide the counts of the target star by an average of nearby comparison stars. A decrease in brightness in the “raw” light curve resulting from a passing cirrus cloud, for example, or from the SOAR telescope pointing so that it is partially obscured by the dome, will be present in all stars in the field of view. Dividing the target by an average of the comparisons will remove this artificial dip.

To first order, the comparison stars also remove the variation in brightness that comes with observing through changing airmass as the elevation of the target field changes. Residual trends with airmass resulting from the color difference between the target and comparison stars will remain, but these variations are on timescales much longer than the variability that concerns us here, so we remove this long-term trend and convert the data to fractional intensity about a mean of zero by dividing by a parabolic fit and subtracting one.

If the S/N is high enough and the amplitude large, variation may be detectable by eye in this light curve. Such is the case for SDSS J2200–0741 as seen in the top panel of Fig. 2.3. However, if a variable signal is too small to be visible above the noise in an individual cycle, we will not see it in the light curve. Averaging over multiple cycles, however, the noise will average to zero and the signal will stand out. A Fourier transform of the data performs just this task, checking all possible frequencies in the data. The resulting amplitude spectrum is a plot of the set of amplitudes and frequencies needed to reconstruct the time-series data with a sum of sinusoids. The bottom panel of Fig. 2.3 shows a light curve of SDSS J2348–0942, which is suggestive of periodic variation, but the amplitude spectrum resulting from the Fourier transform of this data (bottom panel of Fig. 2.4) makes the signal apparent.

A Fourier transform of the SDSS J2200–0741 data reveals two prominent, harmonically-

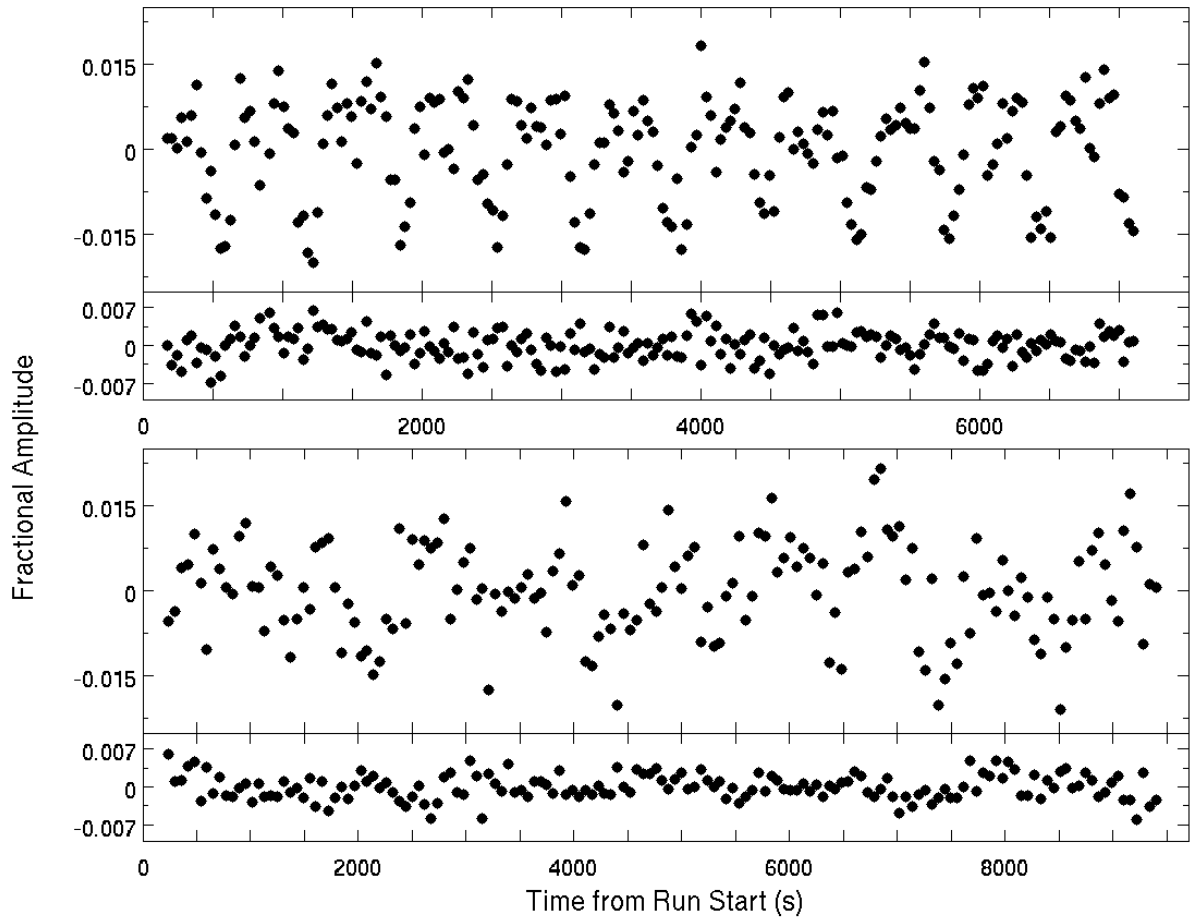


Figure 2.3: Periodic variation is apparent in the light curve of SDSS J2200–0741 (top). While there appears to be scatter above the noise in the light curve of SDSS J2348–0942 (bottom), a Fourier transform is needed to confirm the periodic signal (see Fig. 2.4). The bottom sections of each panel show the light curves of comparison stars.

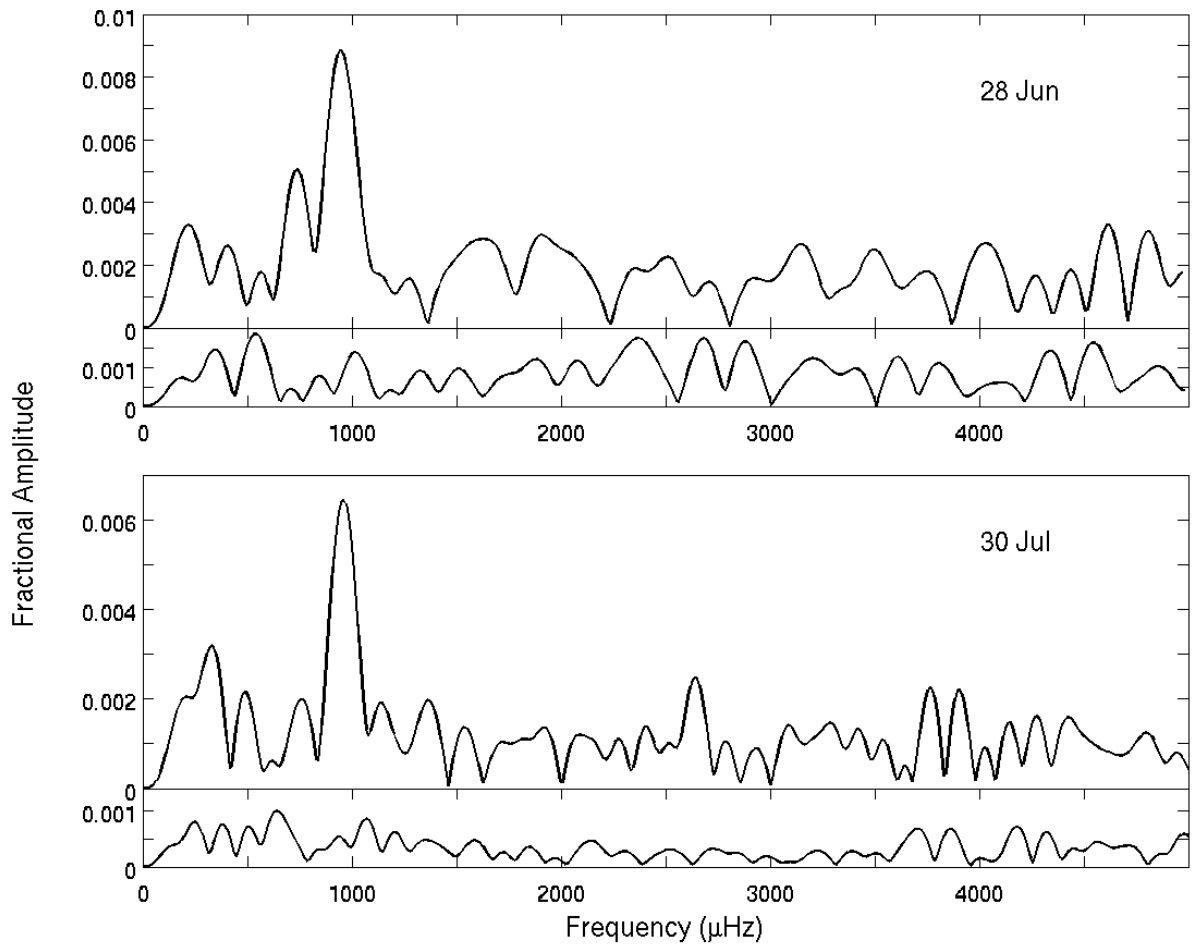


Figure 2.4: The signal near $950\mu\text{Hz}$ is obvious in the amplitude spectra of both sets of SDSS J2348–0942 time-series data. The bottom section shows no significant periodic signal in a nearby comparison star.

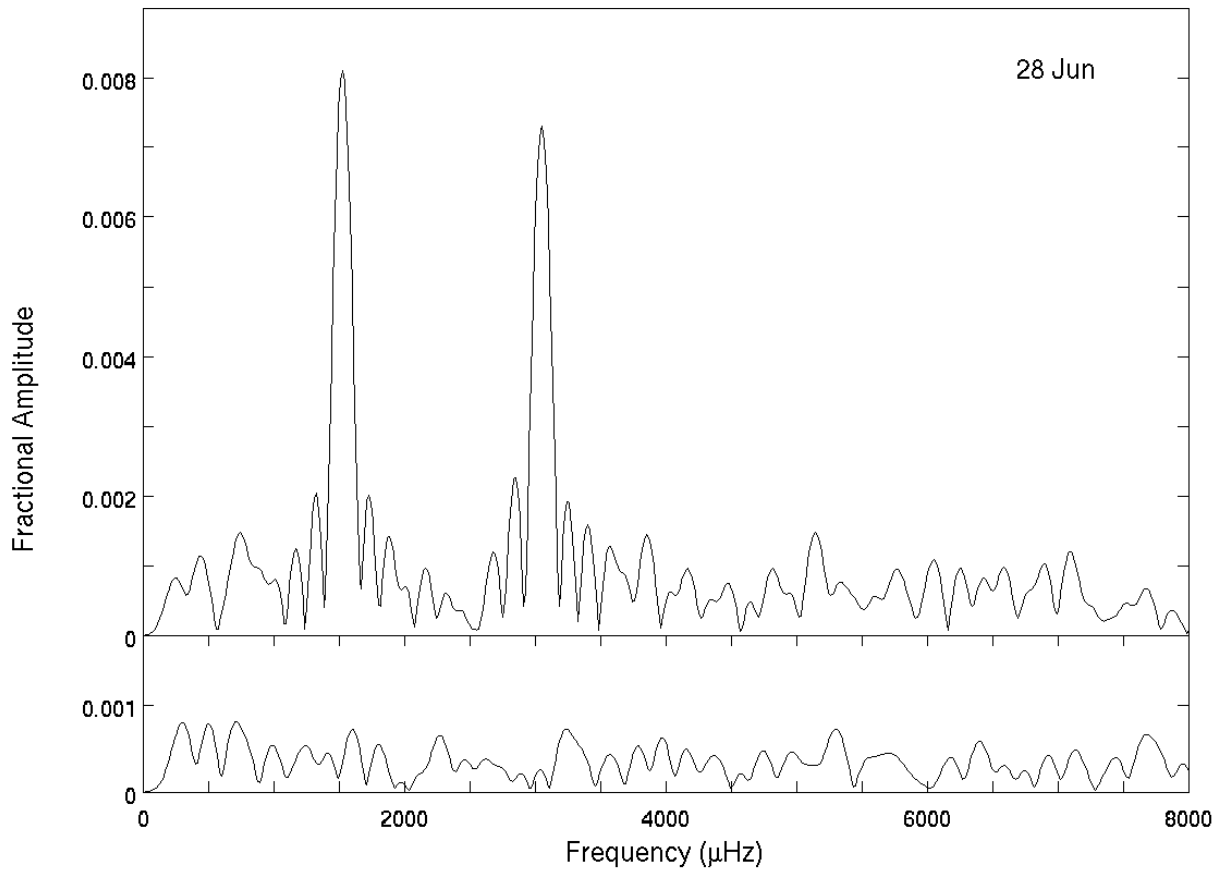


Figure 2.5: The amplitude spectrum of SDSS J2200–0741 displays two prominent peaks resulting from its nonlinear pulse shape.

related peaks (Fig. 2.5). This implies that the variation cannot be modeled as a lone sinusoidal oscillation, yet we refer to the variation as monop periodic since there is one pattern of light modulation that continually repeats at the fundamental period. This is true so long as the peaks in the Fourier transform are all harmonically related. Modeling this variation with a set of sine functions is a convenient way to describe it precisely, but the presence of multiple frequencies in this analysis does not imply, for example, multiple independent pulsation modes. We now turn to this modeling as a way of describing the pulse shape.

Table 2.2: BEST-FIT PARAMETERS FOR SDSS J2200–0741 AND SDSS J2348–0942

Object	UT Date (2008)	Frequency (μHz)	Amplitude (%)	Phase ^a (cycles)
SDSS J2200–0741	27 Jun	1531.2 ± 8.7	0.668 ± 0.075	0.88 ± 0.02
		3053.3 ± 7.1	0.760 ± 0.071	0.48 ± 0.02
	28 Jun	1527.4 ± 6.5	0.804 ± 0.066	0.09 ± 0.01
		3052.9 ± 7.6	0.730 ± 0.070	0.89 ± 0.02
	27 Jul	1512 ± 11	0.740 ± 0.093	0.29 ± 0.02
		3060 ± 11	0.726 ± 0.094	0.41 ± 0.02
SDSS J2348–0942	28 Jun	944 ± 12	0.88 ± 0.13	0.27 ± 0.02
	31 Jul	958 ± 6.7	0.64 ± 0.08	0.38 ± 0.02

^a The uncertainties shown are lower limits.

2.3.2 Pulse Shapes of SDSS J2200–0741 and SDSS J2348–0942

We would like to see what the variation looks like to be able to compare it to the prototype DQV, to white dwarf pulsators, and to known rotating magnetic white dwarfs. Performing non-linear least squares fits of sine waves to the data gives us the best-fit period. This allows us to fold the data on the fundamental period and average points of the same phase to increase S/N so that we can clearly see the shape of the variation. The fitting procedure also provides the relative phases of the fundamental and harmonic. This phase difference tells us whether the light curve is best modeled by, e.g., a harmonic whose minimum lines up with the fundamental minimum (and maximum), which would produce a shape like the prototype DQV. White dwarf pulsators have the opposite relationship, where the harmonic maximum aligns with the fundamental minimum, making it shallower as seen in Fig. 2.2.

For the period analysis we take initial amplitude and frequency guesses from the prominent peaks in the amplitude spectra and then perform non-linear least-squares fits to the time-series data. The results of these fits, which were performed with WQED, are shown in Table 2.2. Then we fold the data on the best-fit period for each night (Fig. 2.6) revealing that SDSS J2200–0741 looks suspiciously similar to the prototype and, thus, distinctly unlike the known white

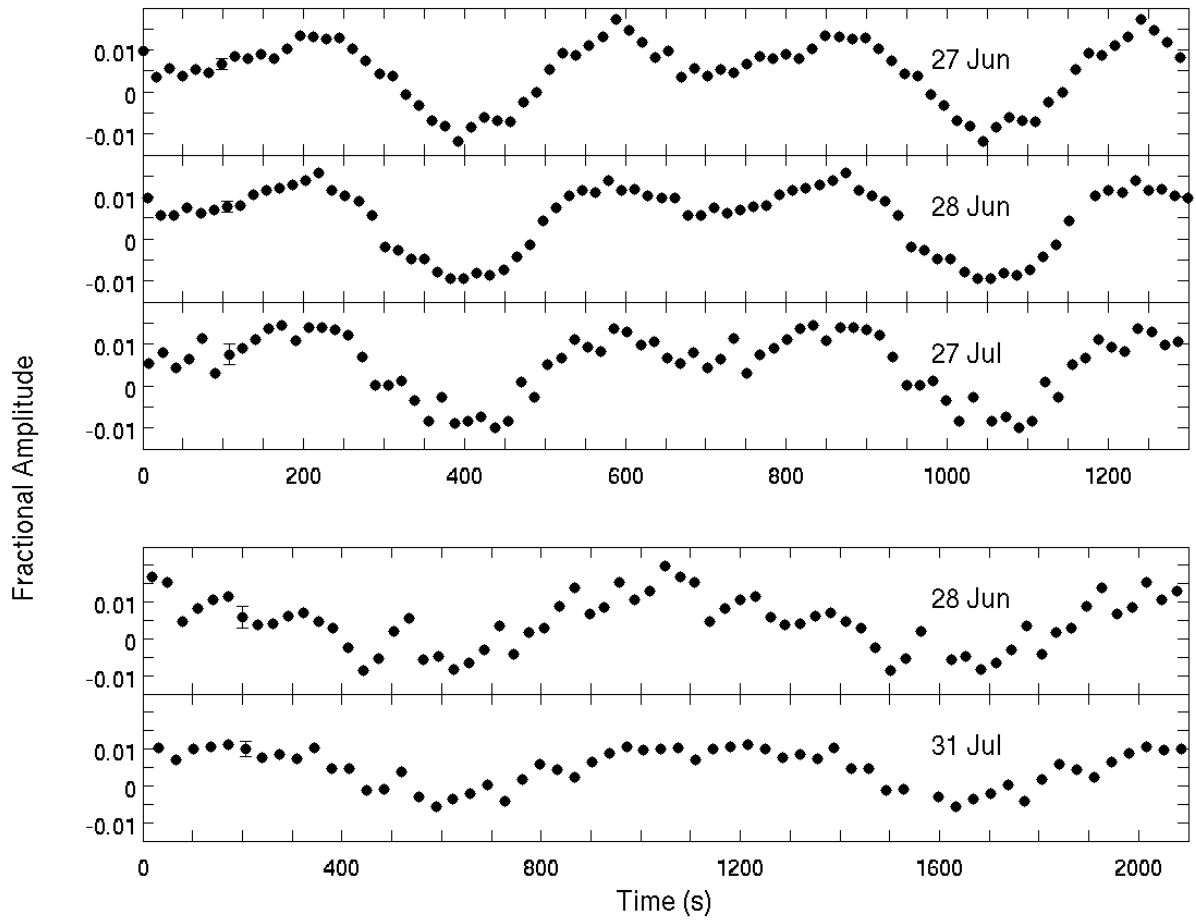


Figure 2.6: The pulse shape of SDSS J2200–0741 (top panel) resembles that of SDSS J1426+5752 (Fig. 2.2) with deep minima and secondary minima in between. To within our detection limits, SDSS J2348–0942 is well-modeled by a simple sinusoidal variation. The data are duplicated across two periods for clarity.

dwarf pulsators. From the phases in Table 2.2 we can compute the phase difference between the fundamental and harmonic. (Phase, ϕ , is defined by the argument of the sin term of the fits, which we chose to be $[2\pi f(t - \phi)]$.) For each night we find that, the harmonic minimum occurs 9–18 s before the fundamental minimum (consistent with 0 s within the errors), which is a small fraction of the period, so, as expected from the pulse shape, these minima are aligned.

Table 2.3: SDSS J1337–0026 OBSERVATION LOG

Date (UTC)	Start Time (UTC)	T_{exp} (s)	T_{cycle} (s)	Length (s)	Airmass	Instrument	Filter	Comparison Stars
2008 Jul 27	00:00:59.4	45	49.5	5939	1.34–2.01	Goodman	none	C1 ^a ,C2 ^b
2009 Apr 20	05:24:24.9	40	44.0	12878	1.19–3.11	Goodman	S8612	C1,C2
2009 Jun 27	23:57:00.3	38	39.9	13390	1.16–2.09	SOI	SDSS g ^c	C1,C2,C3 ^c
2009 Jul 23	23:54:00.4	25	27.9	9947	1.28–2.92	SOI	SDSS g ^c	C1,C2,C3

^a SDSS J13:37:13.17–00:28:33.3, $g'=16.9$, $u'-g'=1.5$

^b SDSS J13:37:12.50–00:26:11.7, $g'=17.0$, $u'-g'=1.2$

^c SDSS J13:37:18.44–00:25:58.3, $g'=17.1$, $u'-g'=1.9$

2.3.3 Observations of SDSS J1337–0026

We now turn to our observations of SDSS J1337–0026, which, besides providing further evidence that a large fraction of the hot DQs are variable, establishes the pulse shape discovered in the prototype as a common feature of DQVs. We first obtained usable data on 2008 July 27. We observed a field containing the target with the Goodman Spectrograph in imaging mode with the CCD readout binned to yield 0.3 arcsec pixels. During the 1.6 hr of unfiltered photometry, the average seeing was 2.8 arcsec and became increasingly unstable. On 2009 April 20, we observed SDSS J1337–0026 for 3.6 hrs with the S8612 filter. The average seeing was 1.3 arcsec, and the second half of the data, as the Moon was rising, shows significant periodic variations in the sky brightness with a period of around 720 s, as might result from passing clouds with periodic structure, or periodic obstruction by the SOAR dome.

The next observing nights presented us with more stable atmospheric conditions. On 2009 June 27, we obtained 3.7 hrs of data through a Sloan g filter using SOI since Goodman was unavailable. The whole chip was read out and binned 6×6 to yield 0.46 arcsec pixels, which oversampled the poor average seeing of 2.5 arcsec. We gathered 2.8 hr of data with SOI on 2009 July 23 with a ~ 5 min gap due to a guiding problem. The 4×4 binning resulted in a plate scale of $0.31 \text{ arcsec pixel}^{-1}$, and the average seeing was 1.1 arcsec. Table 2.3 summarizes these observations.

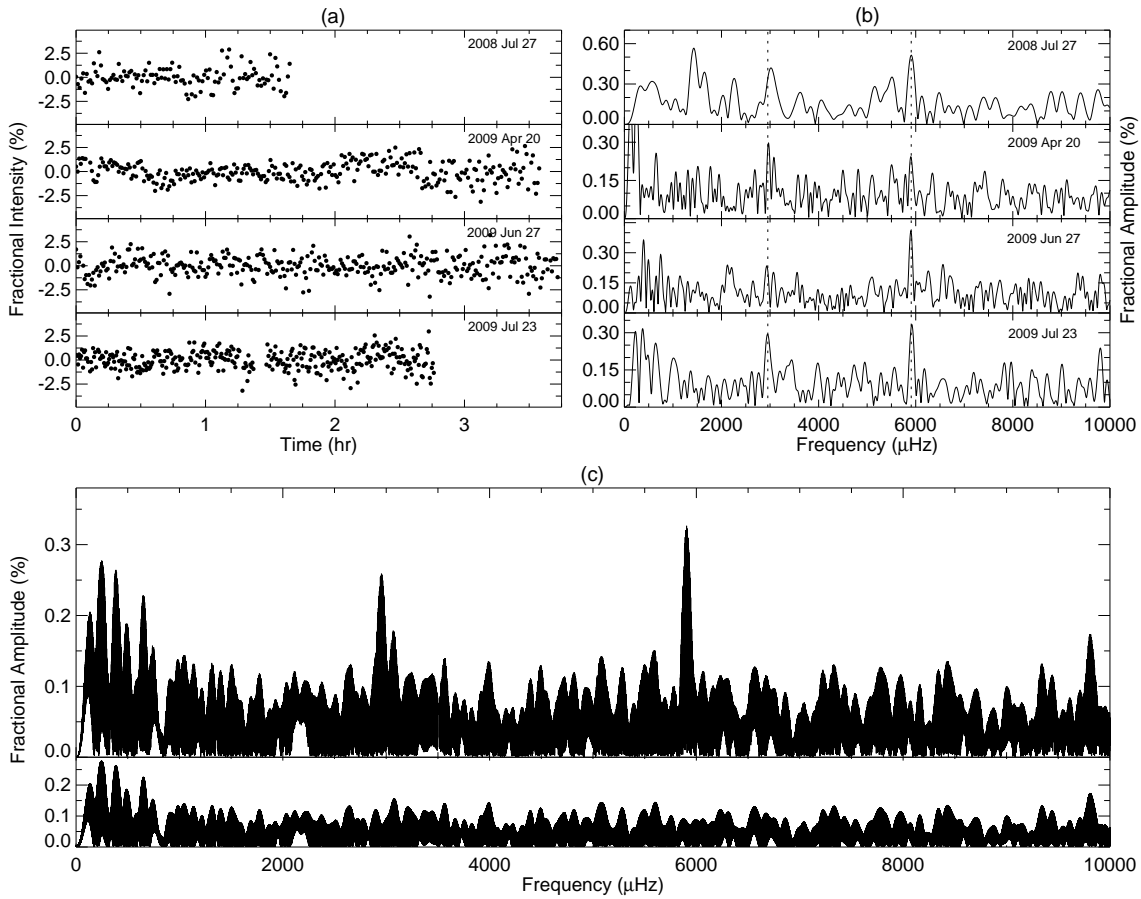


Figure 2.7: We show that SDSS J1337–0026 is photometrically variable with a small amplitude that makes it hard to discern in the individual light curves, but the Fourier transforms show significant variability at two harmonically related frequencies.

We subjected the raw data to the same procedure outlined in § 2.3.1 to create the light curves in Fig. 2.7(a). Though no signal is apparent to the eye in the photometry, the amplitude spectra (Fig. 2.7(b)) produced from discrete Fourier transforms of each of the light curves reveal noticeable signals on all four nights near $5900 \mu\text{Hz}$ (169 s). A peak near the harmonically-related frequency $2950 \mu\text{Hz}$ (339 s) does not always stand out in the nightly amplitude spectra, but the combined 2009 amplitude spectrum shows both to be obviously above the noise (Fig. 2.7(c)). Because of the small amplitude of these peaks, it seems prudent to engage in a more careful assessment of the odds that they could be a noise conspiracy rather than an authentic signal.

Noise and Probabilities

We assess the significance of the peaks from the combined 2009 data using the Lomb-Scargle normalized periodogram (Lomb, 1976; Scargle, 1982) computed by IDL's LNP_TEST (a routine based on `fasper` from Press et al. 1992). The largest peak in the power spectrum produced from the combined 2009 dataset is near $5900\ \mu\text{Hz}$ and has a power of ~ 26 . If we expect from the 2008 data a peak near $\sim 5900\ \mu\text{Hz}$ and consider just this frequency, then the probability calculation is straightforward. When the periodogram is normalized by the sample variance, the distribution of powers is described by the regularized incomplete beta function (Schwarzenberg-Czerny, 1998) from which we find that the probability that a peak as large as the one near $\sim 5900\ \mu\text{Hz}$ would occur *there* by chance is $\sim 3 \times 10^{-12}$.

If, on the other hand, we want to know the false alarm probability, i.e., the odds of a peak so large occurring by chance *somewhere* in the range considered (0 – $11370\ \mu\text{Hz}$, the Nyquist frequency on the April night), then we need to know the number of independent frequencies that serve to increase the probabilistic resources and thus increase the odds of finding a large peak due to noise. A peak in the amplitude spectrum 4 times above the mean level (a commonly-used threshold) may be significant, but not if it is one among a million different frequencies being assessed for significance. The number of independent frequencies relevant to the probability calculation increases as the number of data points in the time series increases. For relatively short continuous data sets with equal exposure times, the number of independent frequencies is roughly equal to the number of data points. For data sets with gaps and variable sampling rates such as ours, the determination of the number of independent frequencies is not as straightforward. In fact the number of independent frequencies that

serve to decrease the significance of a peak can be several times larger than the number of data points. Computations that ignore this will underestimate the ability of noise to produce seemingly significant peaks in an amplitude spectrum.

We follow the method laid out in section 3.4.1 and Appendix B of Cumming et al. (1999) (see also Horne & Baliunas 1986) and perform 10^5 bootstrap Monte Carlo trials. For each trial we compute the power spectrum of a light curve constructed with the same observation times as the original but with the flux values for each time drawn randomly (with replacement) from the original flux values. A fit to the well-sampled, high probability end of the resulting distribution of maximum powers indicates that the number of independent frequencies is ~ 9 times the number of data points (9×961). This results in a false alarm probability of $\sim 3 \times 10^{-8}$ which is a factor of 10 smaller than an extrapolation of the Monte Carlo results. In either case, variability in SDSS J1337–0026 at this frequency is established at the 5σ level at minimum.

We also calculate the odds that a peak as large as the one at $2950 \mu\text{Hz}$ will occur somewhere in the frequency range by chance and find $\sim 0.07\%$ (3.4σ) according to the analytic calculation, or $\sim 0.15\%$ (3.2σ) according to the Monte Carlo results. However, because the $5900 \mu\text{Hz}$ oscillation is firmly established and because many plausible mechanisms for variability give rise to harmonics, given one established frequency, it is typical to look for variability at the location of harmonics. In this case, and because the peak at $2950 \mu\text{Hz}$ is relatively significant on all four nights, we want to know the odds that a peak as large as the one at $2950 \mu\text{Hz}$ will occur *there*, so the probability of a chance occurrence, which is not increased by searching a large number of frequencies, is $\sim 7 \times 10^{-8}$ (5.4σ). We thus consider this harmonically related peak to indicate real variability as well.

Table 2.4: BEST-FIT PARAMETERS FOR SDSS J1337–0026

Period (s)	Frequency (μHz)	Amplitude (%)
2008 Jul 27:		
700.7 ± 9.2	1427 ± 19	0.55 ± 0.11
331.7 ± 2.8	3015 ± 26	0.40 ± 0.11
169.30 ± 0.59	5907 ± 21	0.50 ± 0.11
2009 Apr 20:		
337.0 ± 1.4	2967 ± 12	0.293 ± 0.080
169.49 ± 0.41	5900 ± 14	0.243 ± 0.081
2009 Jun 27:		
340.9 ± 1.6	2933 ± 14	0.232 ± 0.077
169.47 ± 0.22	5900.7 ± 7.8	0.408 ± 0.077
2009 Jul 23:		
338.9 ± 1.5	2950 ± 13	0.288 ± 0.070
168.94 ± 0.33	5919 ± 12	0.329 ± 0.070

2.3.4 Another Odd Pulse Shape in SDSS J1337–0026

Having established the significance of our detection of variability in SDSS J1337–0026, we will now characterize it and assess its stability. Aside from its small amplitude, nothing is clear about the features of its light curve in Fig. 2.7(a), so, as before, we will want to fold the data on the best-fit period and look at the phase relationship of the fundamental and harmonic. We perform non-linear least-squares fits using both Period04 (Lenz & Breger, 2005) and MPFIT (Markwardt, 2009). The largest peak in the 2008 July amplitude spectrum is at approximately half the $2950 \mu\text{Hz}$ frequency but is not significantly present on the subsequent nights, so we include this extra, low-frequency component in the fit for that night only and note that fitting without it does not yield a significant difference. We list the best-fit parameters and their formal errors in Table 2.4.

As we have seen, SDSS J1426+5752 (Fig. 2.2) and SDSS J2200–0741 (Fig. 2.6) have a pulse shape with a deepened minimum and a secondary dip between primary minima. We

have also shown that in reconstructing this with sine waves, the deep minimum results from alignment of the fundamental and harmonic minima. We now proceed to investigate this phase relationship between the fundamental and harmonic in SDSS J1337–0026. We first assume that the two significant frequencies are in fact harmonically related (if they are not, the shape of the light curve does not repeat at the fundamental frequency). To show that this assumption is consistent with the data, we compute a weighted average of the frequencies on the four nights using the inverse variances as weights (Taylor, 1997). This gives $f_1 = 2957 \pm 7 \mu\text{Hz}$ and $f_2 = 5906 \pm 6 \mu\text{Hz}$, which is indeed consistent with $f_2 = 2f_1$.

We refit the data for each night applying this frequency constraint. A weighted average of these results gives $f_1 = 2953.6 \pm 2.7 \mu\text{Hz}$ (338.57 ± 0.30 s); the aliasing in the combined 2009 amplitude spectrum prevents us from confidently determining a more accurate frequency. Consistent with the data, we assume the frequencies are the same on each night and again refit the light curves with the frequencies fixed to look for changes in amplitude and relative phase. Because the flux of the star is changing during an exposure and each measurement represents the average count rate during the exposure, the intrinsic amplitude is diminished by integral sampling. We multiply the best-fit amplitudes and their errors by $\pi T_{\text{exp}} f / \sin(\pi T_{\text{exp}} f)$ to correct for this amplitude-diminishing effect of a finite exposure time, T_{exp} (Baldry, 1999). Table 2.5 lists these results. We report phase difference as the number of seconds between the minimum of the harmonic and the minimum/maximum of the fundamental and use negative values to indicate the harmonic minimum is shifted left of the fundamental minimum/maximum. The one-sigma errors reported for the phase differences come from bootstrap Monte Carlo simulations, and in each case the value falls between the sum of the errors for the individual phases and the quadrature sum of those errors.

Table 2.5: BEST-FIT PARAMETERS WITH $F_1 = 2953.6 \mu\text{Hz}$ & $F_2 = 2F_1$

Date (UTC)	Amplitude _a of f_1 (%)	Amplitude _a of f_2 (%)	Phase Difference (s)
2008 Jul 27	0.35 ± 0.13	0.58 ± 0.14	$+18 \pm 24$
2009 Apr 20	0.28 ± 0.08	0.26 ± 0.09	-12 ± 21
2009 Jun 27	0.22 ± 0.08	0.44 ± 0.08	-47 ± 23
2009 Jul 23	0.29 ± 0.07	0.33 ± 0.07	-1 ± 16

^a The amplitudes and their errors have been multiplied by the factor given in the text to correct for finite exposure times.

By folding the light curves at the 339 s period of the fundamental, we get a picture of these quantitative results (Fig. 2.8). The pulse shape is like those of SDSS J1426+5752 and SDSS J2200–0741. Table 2.5 shows that the harmonic and fundamental minima occur at the same time within the errors. Also, there is no statistically significant change in phase difference or amplitude among the nights.

2.3.5 Pulse Shape Summary

We find the pulse shape of the prototype DQV to be common. Although there is some suggestion that the phase relationship between the fundamental and harmonic might not be exactly zero (corresponding to aligned minima, as we have defined it), the errors in phase are large making small deviations hard to detect. Nonetheless, we note that in all three hot DQs showing harmonics, the best-fit phases tend to be such that the the harmonic minimum comes slightly before that of the fundamental. This is the case in our data on SDSS J1337–0026 and SDSS J2200–0741, in the Montgomery et al. (2008) data on SDSS J1426+5752, and also in the follow-up observations of SDSS J1426+5752 (Green et al., 2009) and SDSS J2200–0741 (Dufour et al., 2009).

Regardless of possible slight misalignments, the phase relationship between fundamental and harmonic is opposite to that of known white dwarf pulsators (as shown in Fig. 2.2 and

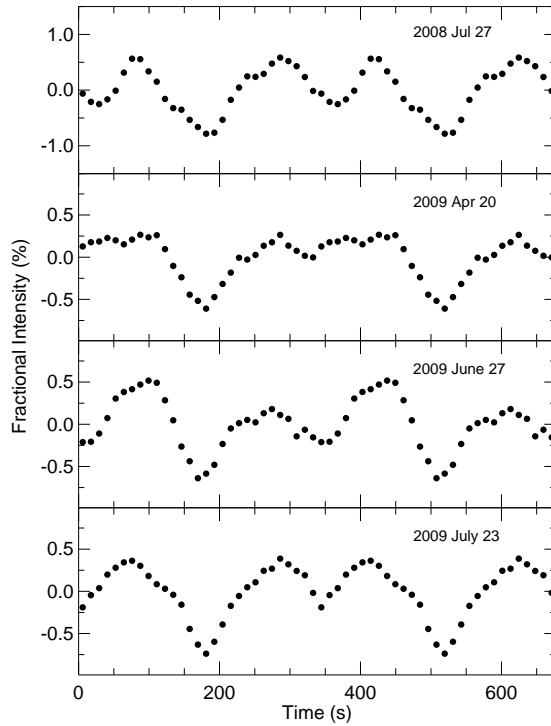


Figure 2.8: The shape of the photometric variation in SDSS J1337–0026 is similar to that of two of the other DQVs as shown here in the pulse shape from four different nights. The data are folded on the main period and plotted twice.

discussed in § 2.3.2). Theories of pulsation in known classes of white dwarf pulsators make specific predictions about such phase relationships (Vuille, 2000; Vuille & Brassard, 2000), so these data permit a potentially important test of models of hot DQ pulsation. However, models of pulsation in magnetic carbon (and oxygen) atmosphere white dwarf stars have not been developed to the point of making such predictions. As an example of pulsators that do display this phase behavior, Green et al. (2009) have pointed to some examples among the roAp stars (magnetic pulsators on the main sequence). If, on the other hand, the variability comes from the rotation of magnetic spots, a variety of pulse shapes can arise from the interplay of field geometry and viewing angle relative to the rotation axis. We will discuss this further in § 2.5.1.

2.4 Other Relevant DQ Observations

Relevant to the question of whether the hot DQs vary because of pulsation or the rotation of magnetic features is the fraction that are variable and also the range of temperature and periods of the variables. The known classes of pulsating white dwarfs pulsate in relatively narrow ranges of temperature. Any theory of hot DQ pulsation will therefore make predictions about which DQs should be variable based on their temperature (and, to a lesser extent, mass). If the DQVs are pulsators, it would be unsurprising if some hot DQs were variable and some were not, but the prediction depends on both the details of the pulsational model and the temperatures and masses of the individual stars. Particular predictions have so far not enjoyed success (Córscico et al., 2009; Fontaine et al., 2008; Montgomery et al., 2008). If variability in the DQs is a result of rotating magnetic features, then a hot DQ at any temperature could be variable so long as it has a magnetic field, and, given that white dwarfs have a wide range of rotation rates, there might be a wide range of periods, unlike white dwarf pulsators, whose observed g -mode pulsations range from ~ 100 – 1500 s.

2.4.1 The DQ NOVs

A large fraction of the hot DQs initially observed turned out to be variable stars, suggesting that most if not all hot DQs are variable. However, we have observed some that we do not observe to vary (NOVs). We present these results in Table 2.6 where we provide the mean noise level in the amplitude spectrum, the size of its largest peak, and an estimate of the false-alarm probability of that peak. Because our observation and analysis strategy has been tuned to search for short-period variations, it is not well-suited to uncovering long-period variability, so in data with formally significant low frequency peaks, we have excluded variations $\gtrsim 1500$ s

Table 2.6: HOT DQS NOT OBSERVED TO VARY

Star	Mean Noise (%)	Largest Peak (%)	False Alarm Probability (%)
SDSS J0005–1002	0.039	0.11	99
SDSS J0106+1513	0.092	0.26	52
SDSS J0236–0734	0.096	0.28	38
SDSS J0818+0102	0.040	0.14	2.0
SDSS J1153+0056	0.065	0.16	98

since these could be artifacts of the way we remove long-term trends in the data.

We note that SDSS J0818+0102 may be variable with a period near 170 s, which we see in at least two nights of data, but we need further confirmation to be confident. Also, though we do not find variability in SDSS J1153+0056, its *HST* UV light curve presented in Dufour et al. (2011a) shows a statistically significant variation. Thus, it appears that only three out of nine hot DQs with high-speed photometry (SDSS J0005–1002, SDSS J0106+1513, and SDSS J0236–0734) do not presently have confirmed or suspected brightness variations. However, we will discuss in the next section the discovery of long-period variation in one of these (SDSS J0005–1002), so we cannot be confident that any hot DQ is photometrically constant.

2.4.2 A Long-Period Hot DQ Variable

In a search for variability among known magnetic white dwarfs, Lawrie et al. (2013) found SDSS J0005–1002 to have a 2.1-day period. Again, we were in a fortunate position to be able to acquire follow-up data quickly. Using data from one of the 0.4-m PROMPT telescopes on Cerro Tololo (Reichart et al., 2005), we have confirmed this discovery. Because this is a long-period variation, it is important to be able to observe the target on multiple, closely-spaced nights, a task for which SOAR is generally not available but to which PROMPT is well-suited. We acquired ~ 10 hr of R-band data with PROMPT, observing during parts of 15 nights over

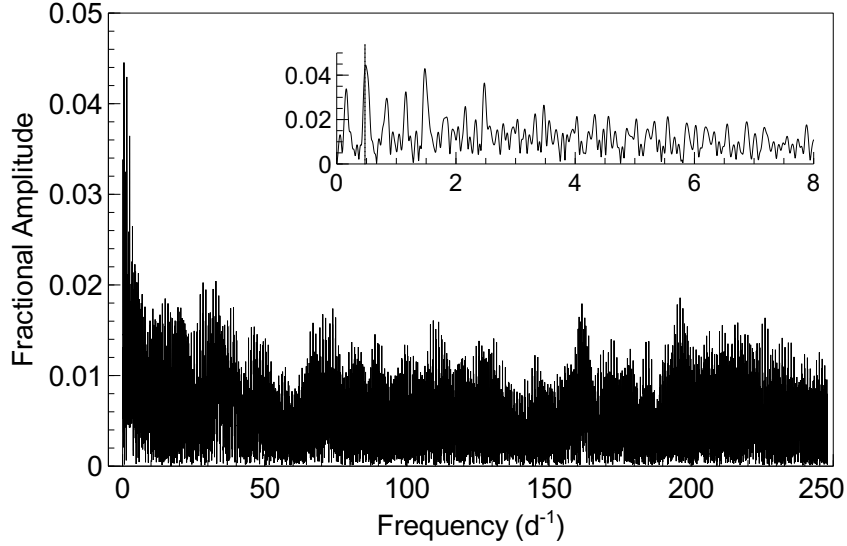


Figure 2.9: SDSS J0005–1002 shows long-period variability as seen in this amplitude spectrum from a discrete Fourier transform of ~ 10 hr of R-band PROMPT data acquired during 15 nights over a span of 19 nights in 2012 Nov. The inset zooms in on the low frequency region where the vertical dotted line marks the frequency corresponding to the 2.11-d period discovered by Lawrie et al. (2013) (the inset axes have the same units as the full plot).

a span of 19 nights in 2012 Nov. The amplitude spectrum of our data (Fig. 2.9) shows a significant peak at the location of the Lawrie et al. (2013) detection. This variability places the NOVs in Table 2.6 in context and suggests an important observational task: all of the hot DQs should be observed for variability on short and long time-scales.

2.4.3 A Warm DQ Variable

Instead of extending the bounds of observed DQ variability in period, the discovered variability in SDSS J1036+6522 by Williams et al. (2013) extends the boundary in temperature. Its variation is sinusoidal like that of SDSS J2348–0942, and it has an almost identical period (1116 s) and similar amplitude (0.4%). Furthermore, like most of the hot DQs, it is magnetic ($B = 3$ MG). However, it is not a hot DQ. Rather, it has C I lines in its spectrum and a temperature near 15,500 K. Thus, it is a “warm DQ,” which, like the cool DQs (Fig. 1.1), has

a helium-rich, rather than a carbon-rich, atmosphere.⁴ Given its temperature and atmospheric composition, there is no theoretical expectation that it would pulsate. However, in the rotating model, the descendants of the hot DQVs should continue to be variable.

2.4.4 Observational Summary

In our attempt to discern the cause of hot DQ variability, we have seen that several are variable and have odd pulse shapes, most are magnetic, and that their variability extends beyond the bounds of temperature and period expected by pulsation. We put these pieces of the hot DQ variable puzzle together in Fig. 2.10. This graphical catalog of photometric variability and magnetism among the DQs immediately shows the prevalence of both phenomena. Also of interest is the number of cases in which the two overlap and where they do not, which we will discuss more below. We point out that just as those with no detected photometric variability may still turn out to be variable, those with no magnetic splitting observed in their spectra may show signatures of magnetism in higher resolution spectra. The high S/N spectra shown in Fig. 1.2 did not indicate magnetism for any of the hot DQs shown there and the top few spectra of Fig. 2.1 are only suspected to be magnetic based on broadened lines, but the magnetic field detection limit of these spectra is ~ 500 kG. Subsequent higher-resolution spectra confirm that SDSS J1104+2035 is magnetic with splittings consistent with a field of ~ 600 kG and indicate that SDSS J1337-0026 also appears to have spectral lines broadened by a magnetic field of around 300 kG (Dufour et al., 2013). The empty spots in Fig. 2.10 are thus currently more of an indication of remaining observational work than a challenge to the magnetic rotator theory.

⁴In this context, it is worth noting that the first DQ variable was the faint ($V=22.2$) cool DQ companion to the millisecond pulsar PSR 0655+64 discovered by van Kerkwijk & Kulkarni (1995) This object shows variability in its C_2 molecular absorption lines that van Kerkwijk & Kulkarni (1995) ascribe to the rotation of magnetic surface features.

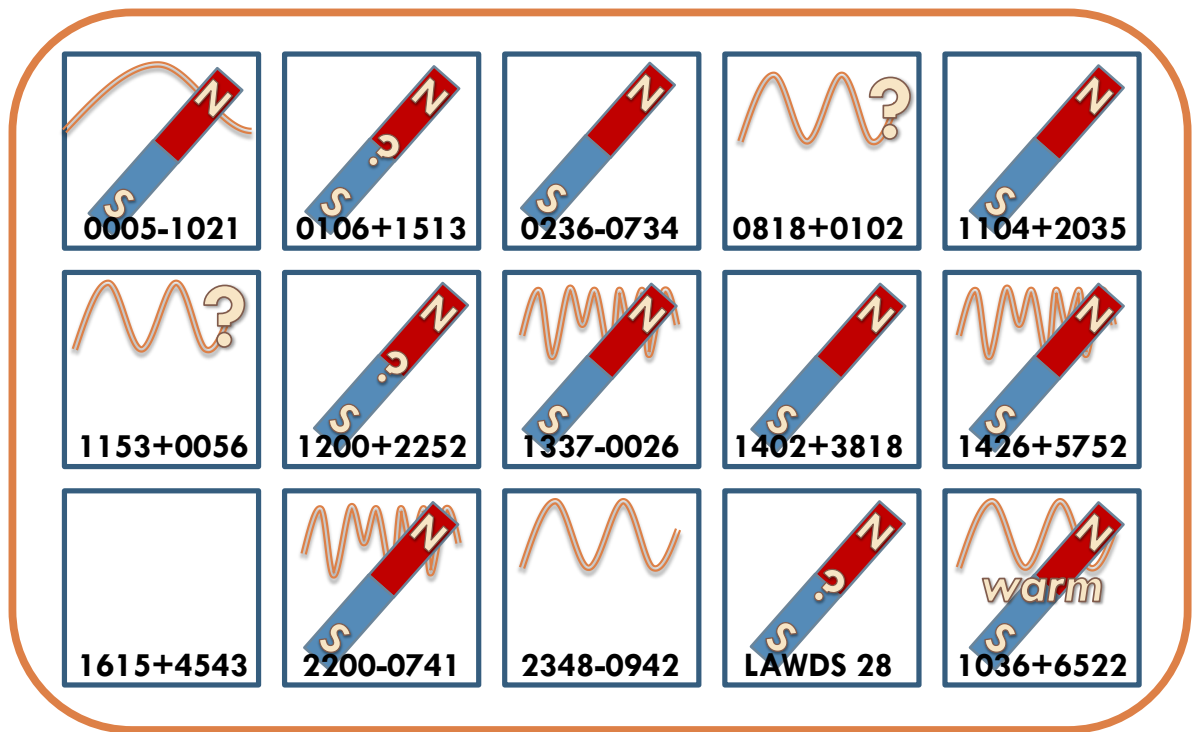


Figure 2.10: Variability and magnetism among the hot DQs. For each star we show whether it is known to be variable (and if so, indicate its pulse shape), suspected to be variable (?), or not known to be variable. We also indicate whether its spectrum shows clear or possible (?) signs of magnetic splitting. The bottom right box represents the warm DQ SDSS J1036+6522.

2.5 Why Do the Hot DQs Vary?

Discerning the cause of a star's variability has been difficult since the early days of stellar astronomy. Goodricke (1786) discovered that δ Cephei was a variable star, and he proposed that the variation was due to rotating star spots. One hundred years later, radial velocity variations discovered in Cepheids were taken to show that their variability was caused by a binary companion (Belopolsky, 1894; Brunt, 1913). In the early 1900s, Shapley (1914) detailed several problems with this explanation, and he and Eddington (1917) proposed intrinsic stellar pulsations (the correct answer) as the cause. In the case of the hot DQ variables, pulsation has been the leading initial hypothesis, binarity was proposed as an alternative explanation early on, and we are here arguing for rotating spots. Apparently, there is nothing new under the Sun.

2.5.1 Pulsation vs. Rotation

The pulsational hypothesis for hot DQ variability has had traction for two reasons. First, they were predicted to be variable based on some straightforward, preliminary pulsational calculations, and, because of this, Montgomery et al. (2008) observed and discovered variability in SDSS J1426+5752. Second, more detailed pulsational analyses of model white dwarfs with carbon-dominated atmospheres show that pulsations are driven in these model stars (Córscico et al., 2009; Fontaine et al., 2008). But reasons to think that they are pulsators based on their actually observed photometric variability are almost wholly absent.

Having expanded the sample of hot DQ variables, we can see that the atypical pulse shape, which first led Montgomery et al. (2008) to question pulsations, is common among the DQVs. We have found that the hot DQ variables have a family resemblance distinct from that of the white dwarf pulsators, and this includes a further distinguishing characteristic:

they are all monoperiodic. This is in stark contrast with all known classes of pulsating white dwarfs (Fontaine & Brassard, 2008b). None of the hot DQs shows a significant frequency that is not harmonically related.⁵ (Those discussed in Green et al. (2009) and Dufour et al. (2009) are marginal detections whose significance would likely decrease in a Monte Carlo analysis, and the possible detections in SDSS J2200–0741 are absent from our data.) Among the hydrogen-atmosphere pulsators, on the other hand, all of the well-studied ones show multiple, independent, periodicities. Only a few—mostly ones having only one or two short data sets—lack multiple independent periods. When a white dwarf is the subject of seismic activity, it is normal, possibly even without exception, to excite multiple modes. Yet, none of the hot DQ photometry shows independent oscillation frequencies.

Such monoperiodic variability is not, however, unknown among white dwarf variables: it is expected and observed in magnetic white dwarf rotators. In particular, we draw attention to the similarity between the characteristic hot DQ pulse shape and the pulse shape of the rotating magnetic white dwarf V471 Tauri. This object spins with a period of 555 s (Clemens et al., 1992), and the shape of its variation bears an uncanny resemblance to that of the DQ variables. V471 Tau has a main-sequence companion that is too far away for direct interaction, but which, nonetheless, showers a light wind of material down on the white dwarf. Because it is channeled by the magnetic field onto the poles, the flux there is redistributed because of absorption at short wavelengths, so the poles are X-ray dim and bright at longer wavelengths.

We expect the hot DQs to be the photonegative of this situation since they presumably have dark spots at the magnetic poles where flux is diminished as the field lines inhibit convective

⁵The presence of harmonics in an amplitude spectrum is not an indication of multiple intrinsic periods but rather an indication that the shape of the repetitive variation at the fundamental period is not sinusoidal.

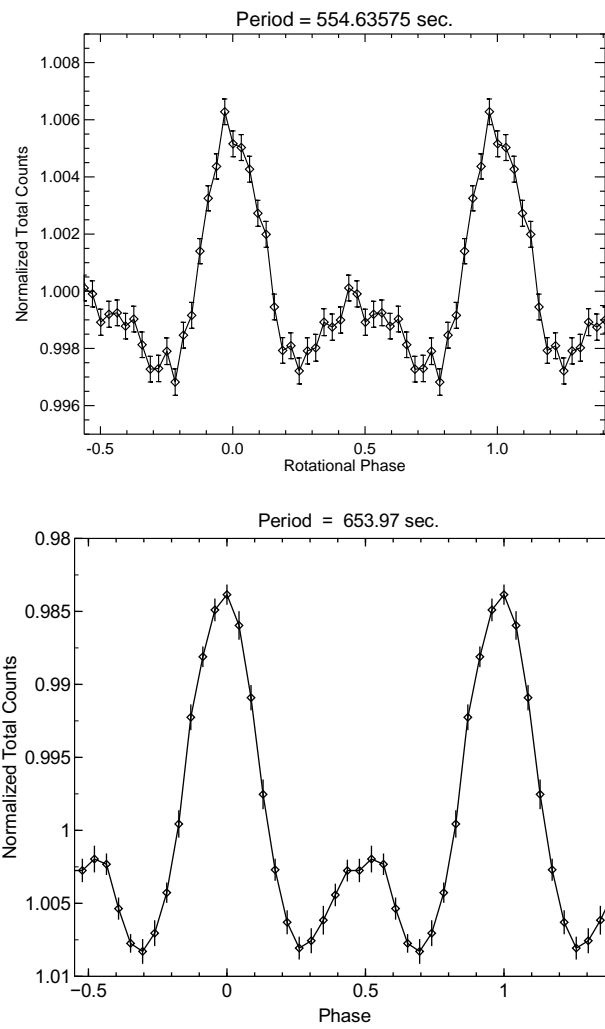


Figure 2.11: The rotating magnetic white dwarf V471 Tau displays photometric variation resulting from the rotation of magnetic spots on its surface (top). The shape of the variation results from the geometry of the magnetic fields and is nearly identical to several of the hot DQ pulse shapes. Because these data are at wavelengths where the magnetic poles of V471 Tau are brighter than the rest of the surface, the pulse shape is inverted from that of the hot DQs, which are presumably darker in their regions of high surface field. Thus, for comparison, we plot the pulse shape of SDSS J2200–0741 upside down (bottom). The top panel is from Sion et al. (2012); reproduced by permission of the AAS.

energy transport beneath the surface. In Fig. 2.11, we show a pulse shape of V471 Tau from Sion et al. (2012). Below it, we plot the pulse shape of SDSS J2200–0741 upside down. Such hot DQ pulse shapes are naturally explained by the presence of two opposite magnetic poles, one darker than the other, that rotate across our line of sight. A more sinusoidal pulse shape could result from just one such magnetic spot rotating around the star.

The discoveries of Lawrie et al. (2013) and Williams et al. (2013) (discussed in § 2.4) provide further support of the rotational hypothesis. The long period variability of SDSS J0005–1002 almost certainly results from the rotation of a magnetic surface feature (or features). It is not physically plausible that pulsations in such compact objects, whose fundamental oscillation periods are ~ 1 s, could have such long periods, and its 2.1-d period is typical for those found in other magnetic white dwarf variables (Brinkworth et al., 2013). Our non-detection of short-period oscillations in the star coupled with this long-period variability are significant. If this hot DQ also displayed rapid variability, then it would not be due to magnetic rotation since the star cannot be rotating at two rates. Short-period variations in this star would thus be a strong piece of evidence in favor of pulsations.

SDSS J1036+6522, the “warm DQ,” shares many properties of the hot DQs: a magnetic field, atmospheric carbon, and photometric variability of similar period and amplitude. Yet it does not share the properties that make the hot DQs theoretical candidates for pulsational instability, namely temperature and carbon-dominated atmosphere. Thus, if one prefers a parsimonious explanation that subsumes all the DQ variability under a common cause, the rotation of surface magnetic features appears to be the only option.

An obvious implication of this is that all of the variable hot DQs are magnetic. A glance at Fig. 2.10 then yields some predictions. SDSS J2348–0942 is magnetic, and this should

result in line splitting detectable in higher-resolution spectroscopic observations and circular polarization detectable with spectropolarimetry (though spectropolarimetric observations that integrate across a large fraction of the period may wash out signatures of this polarization). The same is true of SDSS J1153+0056 and SDSS J0818+0102 if their variability is confirmed. Furthermore, because white dwarfs tend to rotate on observable timescales and because magnetic fields provide a way to detect this rotation, we expect that the magnetic hot DQs with undetected variability will turn out to be variable. For this same reason, if the short-period variations in the hot DQs are from pulsations of the stars, then the magnetic ones should show distinct rotation-related variability at the stars' rotation periods. Conversely, a straightforward prediction of our interpretation is that no such distinct periodicities will be found since the rotational variation has already been detected.

2.6 Where the Photometry Leaves Us

We have presented our discovery of photometric variability in three hot DQ white dwarf stars, establishing them as a new class of variables, and have characterized their properties: short periods (5–20 min), small-amplitudes ($\sim 0.5\%$), and pulse shapes that are either sinusoidal or have deep minima with shallower minima in between. These discoveries and that of Montgomery et al. (2008) have generated several follow-up observations, both ground-based (Dufour et al., 2009; Green et al., 2009) and with *HST* and *Galex* (Dufour et al., 2011a; Williams et al., 2012). Nonetheless, despite these observational efforts, it is not an easy task to decide definitively between pulsations and rotation as the origin of the DQ brightness variations. Though perhaps compelling, the arguments we have presented here in favor of magnetic rotation have, admittedly, been circumstantial.

Furthermore, it could be argued that the magnetic rotation hypothesis complicates the

mystery of the hot DQs more than it clarifies it. If the magnetic rotator interpretation of the data is correct, then the rapid hot DQ variables are among the fastest rotating single white dwarfs yet discovered (Kawaler, 2014). Isolated white dwarfs are much more likely to be found rotating with periods of a day or two, and only one has a period on the order of minutes. This then adds another peculiarity to the list of hot DQ oddities to be explained. As a class they are unique in their atmospheric composition, their high incidence of magnetism, and, if our interpretation is correct, their high rotation rates.

In the next chapter, we will add one more peculiarity to the list, and this one will help us to make sense of them all. White dwarfs are typically close enough to Earth that we can measure their changes in position, and these motions through space not only show us whence they come and whither they go, they tell us how long they have been kicking around in the Galaxy. Following this line of inquiry reveals that the puckish DQVs are lying about their ages, and this makes them party to a much grander mystery. At the end of its investigation, the circumstantial evidence that the variability comes from rotation will be much stronger, the case that they are spun-up merger remnants will be compelling, and all the quirks of the hot DQs will be tied together in a story that both explains them and makes them key witnesses in the investigation of type Ia supernovae.

CHAPTER 3: HOT DQ KINEMATICS¹

“There is something fascinating about science. One gets such wholesale returns of conjecture out of such a trifling investment of fact.”

—Mark Twain

Attending to the motions of stars is a subtle business. This is not because their actual movements through space are small but because from our vantage at a great distance, their apparent motions are imperceptible. Nonetheless, accurate position measurements at multiple moments over a sufficiently long time allow us to infer that many stars have indeed moved while we were not looking. And their manner of roaming through the galaxy is revealing.

3.1 Mergers and Massive White Dwarfs

The extremely bright explosions of white dwarf stars as type Ia supernovae are the most important luminosity standards for measuring cosmological distances, and a lynchpin for establishing that the expansion of the universe has accelerated (Perlmutter et al., 1999; Riess et al., 1998). In the classical progenitor scenario, a white dwarf gradually accumulates mass from a non-white dwarf companion until its central density is high enough to trigger a thermonuclear runaway (Whelan & Iben, 1973). Yet there appears to be a dearth of such systems tuned to explode (van Kerkwijk et al., 2010). We have suggested that the hot DQ stars have properties consistent with being created by the merger of two white dwarfs, which may be

¹This chapter is a version of a paper soon to be submitted with authors Bart H. Dunlap, J. C. Clemens, P. Dufour, Hugh C. Harris, Conard C. Dahn, and J. P. Subasavage. A version of the main argument has been submitted for publication in the conference proceedings of the 19th European White Dwarf Workshop with authors Bart H. Dunlap and J. C. Clemens

the common route to making type Ia supernovae (Iben & Tutukov, 1984; Maoz et al., 2014; Webbink, 1984). Observations indicate the WD+WD merger rate is as high as the type Ia supernova rate (Badenes & Maoz, 2012). However, simulations have not established which mergers will explode and which have other fates.

In this chapter we will show that the carbon-dominated atmosphere white dwarf stars (the hot DQs) are likely remnants of the merging of two white dwarfs that might have exploded as type Ia supernovae but did not. By considering their kinematics, we will uncover a conflict between two hot DQ age determinations: their temperatures and masses suggest they are relatively young, while their space velocities are those of an older population. This conundrum is most easily solved if they are old stars recently reheated in a merger event.

3.1.1 The Mass Distribution of White Dwarf Stars

As discussed in chapter 1, white dwarfs are the remnants produced by the majority of stars in the universe when they exhaust their nuclear fuel and, after substantial mass loss, leave behind compact, electron-degenerate stars. In Fig. 3.1 we show that these stars have a very narrow distribution of observed masses. The mass-loss process converts a wide range of initial masses into a narrow distribution of white dwarf masses, with more massive stars producing more massive white dwarfs (Koester et al., 1979; Weidemann & Koester, 1984).

The high-mass white dwarfs in samples of H-atmosphere white dwarfs such as the one in Fig. 3.1 are sometimes attributed to mergers (Kleinman et al., 2013; Liebert et al., 2005). However, their number is entirely consistent with the number expected to form from high-mass single stars (Ferrario et al., 2005; Wegg & Phinney, 2012), leaving no obvious population of stars as the expected massive WD merger remnants, which, as “failed type Ia supernovae,” would contain valuable information about the same violent process that ends in explosion.

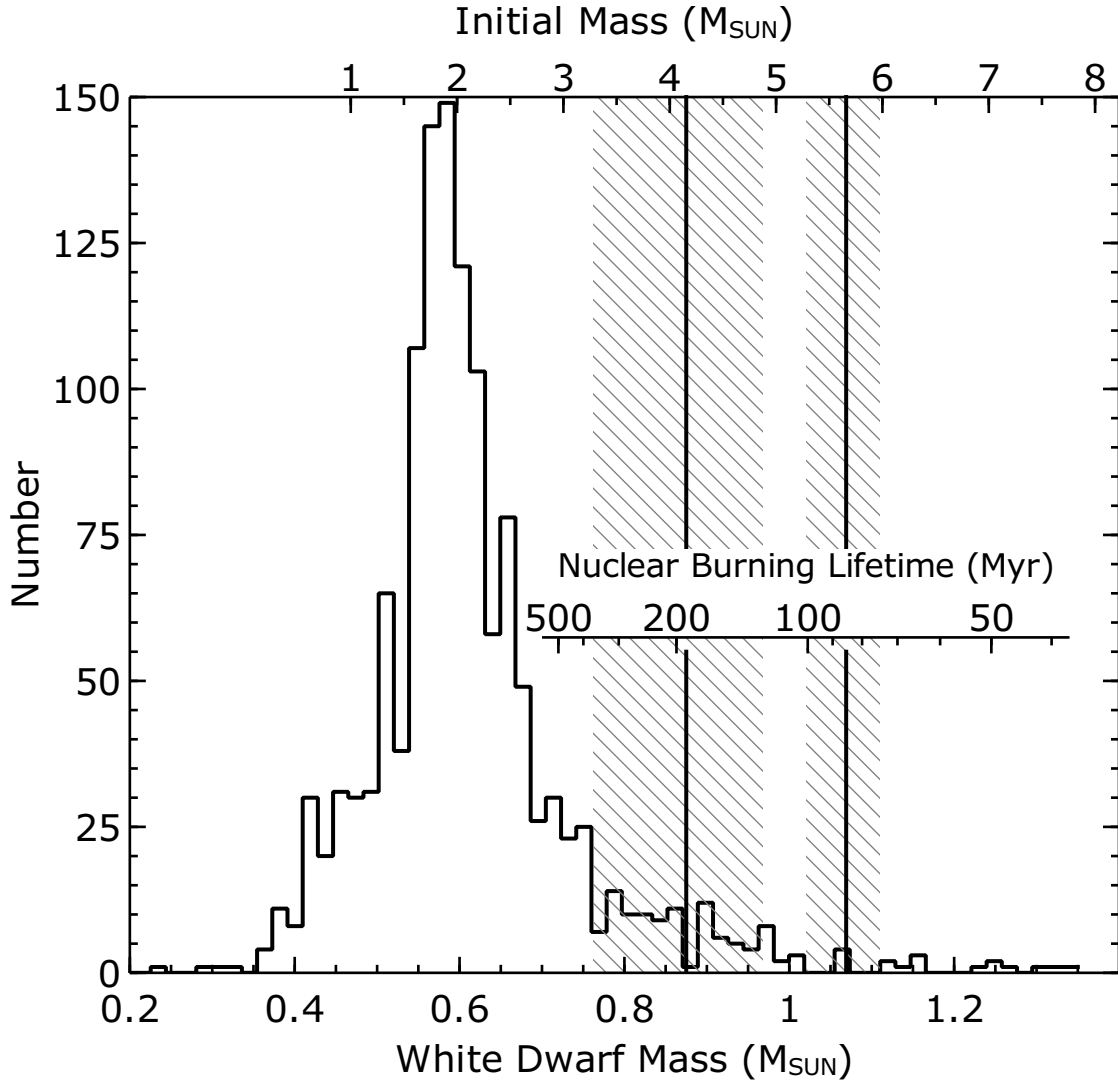


Figure 3.1: White dwarf stars have a fairly narrow mass range centered on $0.6 M_{\odot}$. The two hot DQ white dwarfs with well-determined masses (vertical lines) fall on the high-mass tail of this distribution. If they descended from single stars, those stars were massive (top axis) and short-lived (inset axis), in contradiction with their age from space motions (see Fig. 3.5). The mass distribution includes all 1306 SDSS DR4 hydrogen-atmosphere white dwarfs with well-determined spectroscopic masses (i.e., $S/N > 12$, temperatures between 13,000 K and 40,000 K, and without flags; Tremblay et al. 2011).

3.1.2 Hot DQ Masses

We here consider whether the hot DQ stars might be the missing high-mass population of mergers that did not explode, but first we must find a way to measure their masses. White dwarf masses are normally inferred from temperatures and surface gravities via a theoretical mass-radius relationship. For determining hot DQ masses, however, this method is currently dubious because the input physics for the carbon-atmosphere models is not in a state that allows reliable surface gravity determination from spectral lines (Dufour et al., 2011b). However, it is possible to determine the photometric effective temperature, T_{eff} , from the photometric colors of an object. This temperature largely determines the model surface flux, F_{λ} . The observed flux is just this model flux diminished by a factor of $(R/D)^2$, where R is the stellar radius and D is its distance from Earth. Thus, if we know the distance, we can then determine the radius, and the mass-radius relationship, which is well-determined for electron-degenerate objects, gives us the mass.

We have obtained distances via parallaxes from collaborators at the US Naval Observatory for two hot DQ stars and have combined these with temperatures derived from fitting C-atmosphere models to the observed SDSS photometric flux² to infer masses. Table 3.1 shows the measured and derived parameters. The vertical lines on Fig. 3.1 show that both of these masses are much higher than the mean, as might be expected for merger products.

3.1.3 Massive Hot White Dwarfs are Young

Although these high masses are consistent with merger remnants, because massive white dwarfs also descend from massive single stars, they do not rule out a late He shell flash scenario.

²Models and photometric fits courtesy of P. Dufour. The fitting technique is described in §5.1 of Bergeron et al. (1997).

Table 3.1: PROPERTIES OF THE TWO HOT DQs WITH PARALLAX MEASUREMENTS^a

Parameter	SDSS J2200–0741	SDSS J0005–1002
Absolute parallax (mas)	4.2 ± 0.5	6.2 ± 0.4
Relative proper motion (mas yr ⁻¹)	24.7 ± 0.2	82.9 ± 0.1
Position angle (deg)	286.1 ± 0.4	67.4 ± 0.1
Distance (pc)	239 ± 30	161 ± 11
T_{eff} (K)	$22,370 \pm 1,270$	$19,580 \pm 920$
Radius (R_{\odot})	0.0093 ± 0.001	0.0071 ± 0.0005
Surface gravity (log[cm s ⁻²])	8.44 ± 0.17	8.76 ± 0.08
Mass (M_{\odot})	0.88 ± 0.1	1.07 ± 0.05

^aThe parallax data for SDSS J0005–1002 were acquired over a 7.10-yr baseline (112 frames, 97 nights) and those for SDSS J2200–0741 over a 6.24-yr baseline (126 frames, 91 nights) and were analyzed following the standard USNO procedures (Dahn et al., 2002).

However, if the hot DQs are descended from high-mass single stars, those stars had very short nuclear burning lifetimes. The time a star spends burning its nuclear fuel prior to becoming a white dwarf is roughly proportional to $M^{-2.8}$, so the lifetimes drop sharply at higher mass. The mass of a white dwarf can be used to infer its progenitor mass assuming typical single-star evolution. We use an initial-final mass relationship derived from observations of stellar clusters (Williams et al., 2009):

$$M_{\text{MS}} = (M_{\text{WD}} - 0.339)/0.129$$

We show this main-sequence progenitor mass in Fig. 3.1 (top axis). Then, we find the nuclear burning lifetime (taken to be the end of the AGB phase for most stars, or the onset of carbon burning for the most massive models) of the progenitor using $Z = 0.03$ stellar models³ (Girardi et al., 2000). The result of this calculation tells us how long a white dwarf of a given mass was in the Galactic disk before it became a white dwarf (Fig. 3.1 inset axis).

In addition to the short main-sequence lifetime required by high masses, the high temperatures measured for the hot DQs require that they also have short white dwarf cooling

³Less metal-rich models have shorter lifetimes.

ages (Fontaine et al., 2001). The *total* lifetime of hot, high-mass white dwarfs in the range $0.9 < M/M_{\odot} < 1.2$ is only 250 Myr to 400 Myr *if* they are formed through typical single-star evolution.

3.2 Population Kinematics

“Early in the study of stellar populations—in fact before the term ‘stellar populations’ was invented—a mysterious but significant correlation was discovered. Stars of different astrophysical characteristics showed a different kinematical behavior within the galaxy” (Schwarzschild, 1958). In the Milky Way, stars of recent formation, like hot, massive white dwarfs that evolved from single-stars, have motions similar to the circulating gas from which they formed. Over time, as they traverse the Galaxy, they are stirred up (kinematically heated) by gravitational interactions (Aumer & Binney, 2009). Figure 3.2 shows a model of the resulting increase in velocity dispersion of a population of stars in the Galaxy. As stars become white dwarfs and begin to cool, they continue to be kinematically heated. The velocity dispersion of the population thus serves as a chronometer independent of cooling age and mass.

The young age derived in the previous section for the hot DQ stars from MS lifetime + WD cooling predicts that their kinematic properties should be that of young disk stars with small velocity dispersions if they are formed from high-mass single stars. If, on the other hand, they are massive because they are the result of a merger, the pair of less-massive stars that merged would have lived longer on the main sequence and could have cooled as white dwarfs for a long time before merging. During this time, they will continue to experience kinematic heating. Thus if the hot DQ stars are a population of older white dwarf stars reheated recently in a merger, their velocity dispersions will reflect this history.

As evidence that white dwarfs with different total ages do indeed have distinct velocity

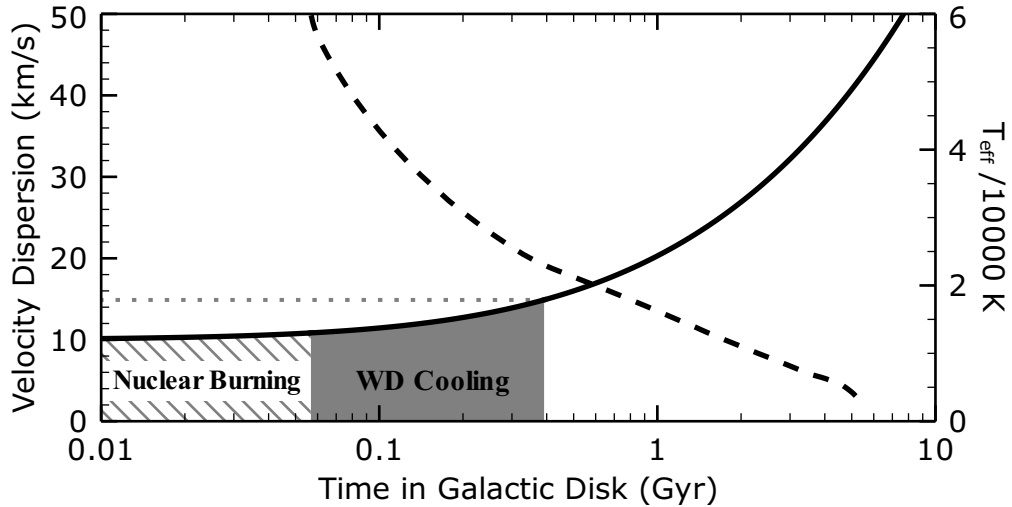


Figure 3.2: A group of hot, high-mass white dwarfs descending from single stars has a small velocity dispersion. A population of stars born in the disk of the Milky Way will be perturbed over time, so its velocity dispersion increases (solid line, left axis, Just & Jahreiß 2010). As white dwarfs cool (dashed line, right axis, Fontaine et al. 2001) their velocity dispersion continues to increase. Here we assume $6.7 M_{\odot}$ progenitors and $1.2 M_{\odot}$ white dwarfs cooling to hot DQ temperatures ($\sim 23,000$ K).

distributions, we show in Fig. 3.3 the transverse (perpendicular to our line of sight) velocity distributions of three sets of white dwarfs grouped by mass (Wegg & Phinney, 2012). Because these white dwarfs were selected to have short white dwarf cooling times, the massive ones have young total ages because they descended from massive, short-lived main sequence stars whereas the lower-mass group lived for much longer on the main sequence.

3.3 What the Motions of the Hot DQs Reveal

Pursuing the idea that kinematics might settle the nature of the hot DQs, we first consider one whose motion is extreme. SDSS J1153+0056 has the largest proper motion of any known hot DQ, $\mu = 153 \pm 4 \text{ mas yr}^{-1}$ (Munn et al., 2004). Even if we feign complete ignorance of its mass, radius, and distance, we can explore its kinematics under a range of assumed masses. For this exercise, we determine its absolute magnitude from He-atmosphere models⁴

⁴<http://www.astro.umontreal.ca/~bergeron/CoolingModels>

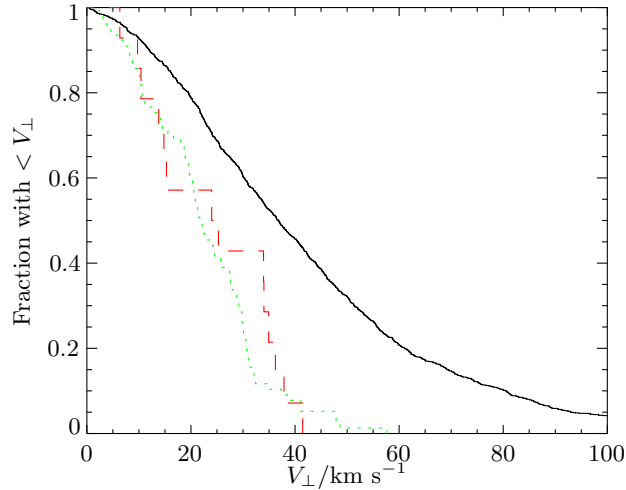


Figure 3.3: White dwarfs of different mass have different transverse velocity distributions. This result is expected for this sample, which is selected to have relatively short white dwarf cooling times, so the typical-mass white dwarfs ($0.5 \leq M/M_{\odot} < 0.75$, black line) come from relatively long-lived main-sequence stars, so their total age is old. The higher mass white dwarfs ($0.75 \leq M/M_{\odot} < 0.95$, green dotted line, and $M > 0.95 M_{\odot}$, red dashed line) have spent much less total time being kinematically perturbed in the Galaxy. The sample consists of more than 1,000 H-atmosphere white dwarfs in the Palomar-Green survey and the SDSS DR4 with cooling ages < 300 Myr. Figure 4 of "White dwarf kinematics versus mass" (Wegg & Phinney, 2012).

(Bergeron et al. 2011; Holberg & Bergeron 2006; The distance and thus velocity errors resulting from using He-atmosphere rather than C-atmosphere models will be $\sim 5\text{--}10\%$). The observed apparent magnitude then gives us a distance, which, with the observed proper motion, yields the velocity perpendicular to our line of sight ($v_{\text{trans}} \propto D\mu$). This transverse velocity then determines how likely the star is to be a member of the Galactic halo, thick disk, or thin disk (Bensby et al., 2003). These membership probabilities are based on samples of stars that have measured kinematics and can also be assigned population memberships based on spectroscopic determinations of temperature, gravity, and metallicity. These probabilities (Fig. 3.4) show that SDSS J1153+0056 has kinematics that place it among an old stellar population (halo or thick disk) for a large range of assumed masses. Yet for most of this mass range, it cannot be a

member of these old populations since its mass and temperature imply a younger age.⁵ This dilemma is resolved if it was reheated in a merger.

Having established that SDSS J1153+0056 has a very old kinematic age and a much younger WD cooling + MS age (assuming single-star evolution), we now consider the velocities of the hot DQs as a group. We will compare the cumulative distribution of transverse velocities for the whole population to simulations of white dwarf populations, specifically, a young massive population and an older merger population. Fortunately, these simulated distributions have been published (Wegg & Phinney, 2012). Given the difference in velocity dispersion observed for white dwarf populations of different age in Fig. 3.3, it is not surprising that the theoretical simulations of the kinematics expected for a population of reheated white dwarf merger remnants show measurably broader velocity distributions than those of single massive white dwarfs descending from massive main sequence stars (Wegg & Phinney, 2012). These simulated distributions can be compared to the hot DQ stars under the assumption that the masses we have determined for two members are typical for the whole spectroscopic class. While we cannot be certain all hot DQs are massive, the two chosen for parallax measurements were the brightest two of the nine hot DQs known at the time. Because less massive white dwarfs are intrinsically larger and thus brighter, choosing the brightest objects introduces a bias towards probing the lower-mass objects among the group. Given that two of nine are on the high-mass extreme of the overall white dwarf mass distribution, it is likely that the hot DQs as a whole are massive.

⁵The kinematic data do not rule out the possibility that SDSS J1153+0056 is a low-mass halo white dwarf. We find this unlikely given the similarity among hot DQ properties and the masses of the two with parallax measurements. We also note that the late He flash single-star evolutionary scenario for hot DQ formation requires that they be massive (Althaus et al., 2009), so SDSS J1153+0056 (and the group kinematics we discuss below) provides a *reductio ad absurdum* for this scenario.

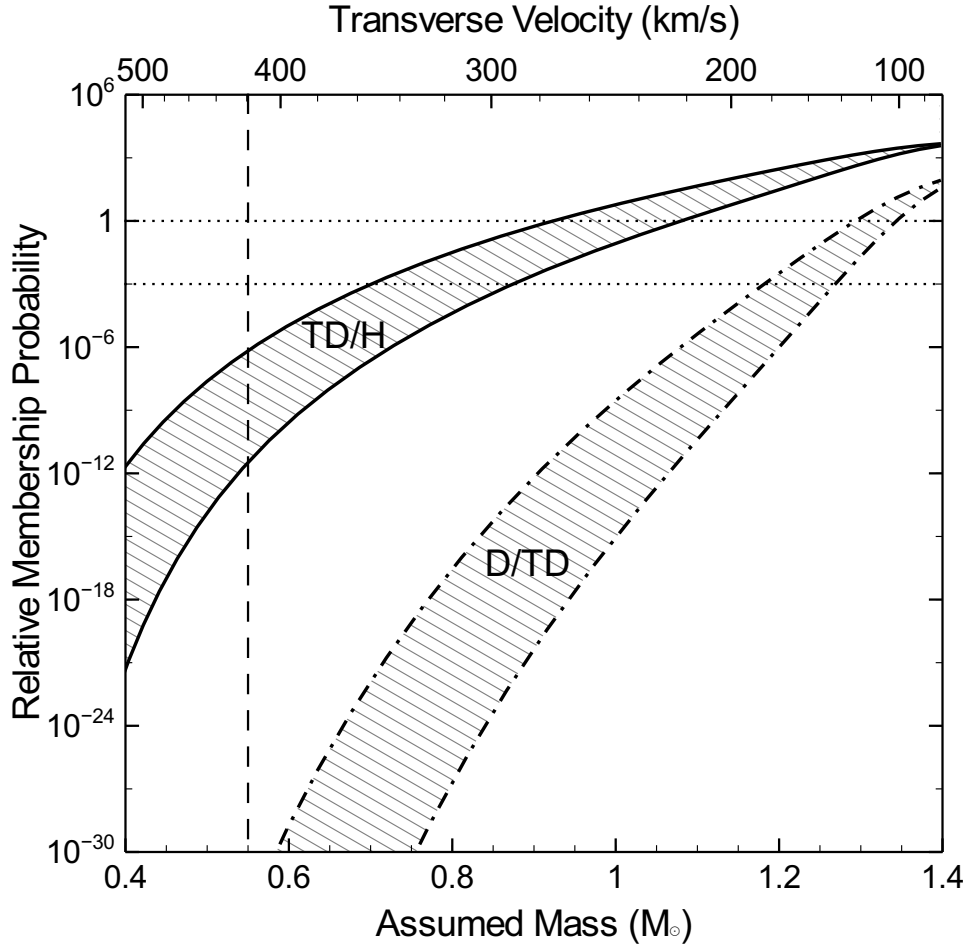


Figure 3.4: SDSS J1153+0056 has no comfortable home where its cooling age is compatible with the age of its likely kinematic population. The upper region shows its thick disk-to-halo (TD/H) probability ratio (where TD/H > 1 means it is more likely to be in the thick disk than halo). The lower and upper solid lines bound the DQ temperature range (26,000 K–18,000 K). The lower region shows the disk-to-thick disk (D/TD) probability ratio with the same boundaries (dot-dashed lines). If its mass is below $\sim 1 M_{\odot}$, SDSS J1153+0056 has a large radius and higher luminosity, requiring that it lie at greater distance. But for such distances the high proper motion implies truly impressive transverse velocity (top axis). For velocities this high, it is more likely to be in the halo than the thick disk, but halo white dwarfs at these temperatures are $\lesssim 0.55 M_{\odot}$ (vertical dashed line) because they come from relatively low mass stars; the higher-mass halo stars long ago became white dwarfs, which are now cooler. Between ~ 1 and $1.2 M_{\odot}$, it has thick disk kinematics, but again it is too massive for that population given its temperature.

To compare the hot DQ kinematics with simulations, we have assembled published proper motions (Munn et al., 2004) for the 13 hot DQs identified in SDSS DR7 (Kleinman et al., 2013) and converted them to transverse velocities. For those without parallax measurements, we assume $\log g = 8.5$ ($M \approx 0.92 M_{\odot}$) and determine temperature based on fits of C-atmosphere models to the SDSS photometry.⁶ The assumed surface gravity and mass-radius relationship give us the radius, and the distance is then found using the inverse of the above relationships used to find mass (§3.1.2). Fig. 3.5 shows that the cumulative hot DQ transverse velocity distribution is broad like the model merger population, which assumes merger remnants with masses between 0.95 and $1.2 M_{\odot}$. If the hot DQs have a similar range of masses, they will fall closer to the model merger line. Their velocity dispersion shows evidence of significant kinematic heating, which is entirely inconsistent with that expected for high-mass white dwarfs evolved from single stars.

We can also compare this distribution of velocities to the 67 white dwarfs in Fig. 3.3 with $M > 0.75 M_{\odot}$ and see that the velocity dispersion of the hot DQs is inconsistent with the observed population of hot, high-mass white dwarf stars. None of these has a transverse velocity greater than 60 km s^{-1} (fewer than 5% have $v_{\text{trans}} > 40 \text{ km s}^{-1}$). Yet in the sample of only 13 hot DQ white dwarfs, at least SDSS J0005–1002 and SDSS J1153+0056 have transverse velocities greater than 60 km s^{-1} , and there is a significant tail beyond 40 km s^{-1} . If we assumed the hot DQs had masses more like the intermediate group in Fig. 3.3 ($0.75 \leq M/M_{\odot} < 0.95$), then their velocities would be even higher, and thus would be more at variance with the observed population of comparable mass.

⁶Courtesy of P. Dufour

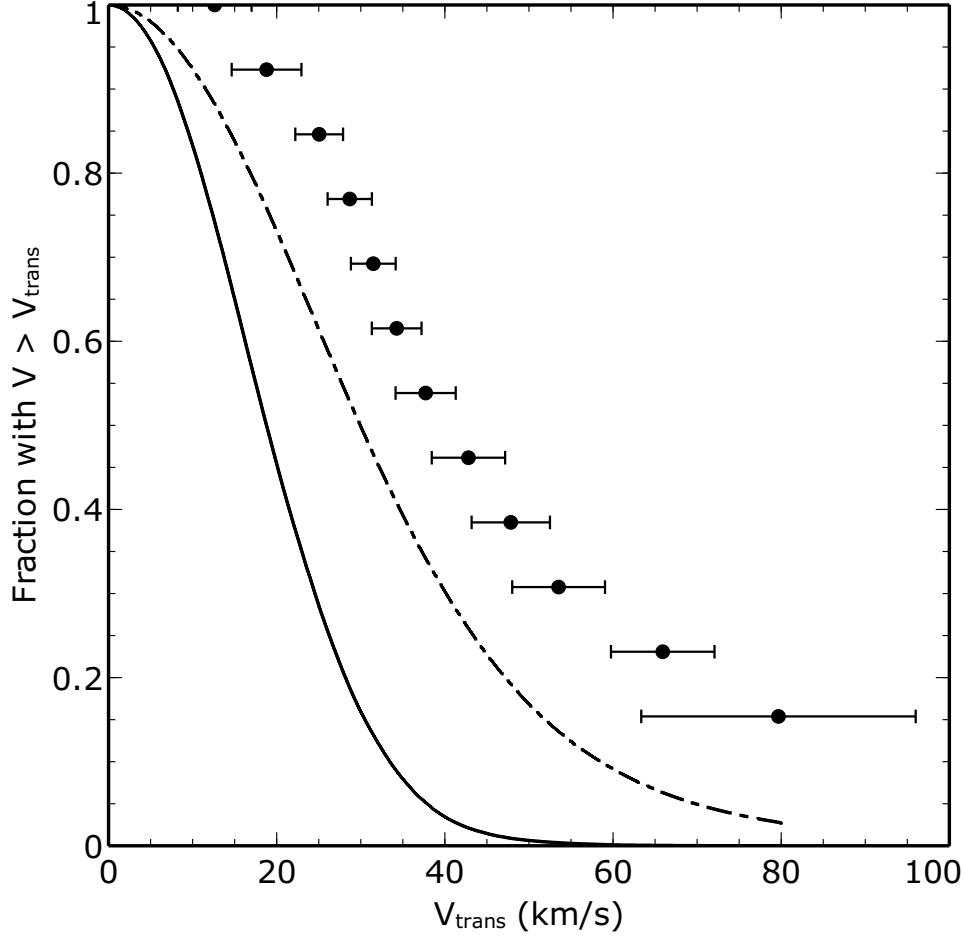


Figure 3.5: Cumulative distribution of hot DQ transverse velocities compared to theoretical simulations (Wegg & Phinney, 2012) for massive ($0.95\text{--}1.2 M_{\odot}$) white dwarfs evolved from single stars (solid line) with cooling ages < 300 Myr (so young total age; see Fig. 3.1), and massive white dwarfs produced in mergers (dot-dashed line), an older population. The distances to hot DQs without parallaxes are determined by assuming $\log g = 8.5$ ($M_{\text{DQ}} \approx 0.92 M_{\odot}$). Like the mergers in the simulation, the hot DQs have transverse velocities indicative of an older stellar population whose space motions have been perturbed over time by gravitational interactions in the disk. Velocity error bars were determined by 10^6 Monte Carlo trials that take into account the 1 s.d. errors in the proper motions and temperatures. One point is off the plot at (286 km s^{-1} , 0.077) because of the extreme velocity of SDSS J1153+0056.

In a further comparison with observed white dwarf kinematics, Fig. 3.6 shows the U and V velocities of a sample of 371 white dwarfs from Farihi et al. (2005). We define U to be positive in the direction of the Galactic center (the opposite sign convention from Farihi et al. 2005), and V is positive in the direction of Galactic rotation. We calculate U and V using the method in Johnson & Soderblom (1987) and take the value of the north Galactic pole from the Appendix of Reid & Brunthaler (2004). We also show 2σ velocity boundaries of thin and thick disk stars (Bensby et al., 2003). Yet again, SDSS J1153+0056 is an extreme outlier regardless of assumed mass. SDSS J0005–1002 also finds itself on the outskirts of the observed distribution, unlike a young star, which would be near the center. In the sample of Farihi et al. (2005), 10% of the stars have white dwarf cooling ages greater than 1 Gyr, and many likely have total ages of a few billion years. Even in such a diverse sample, the hot DQs display distinct kinematics.

As a final note on the motions of hot DQs, we draw attention to NGC 2168:LAWDS 28, a hot DQ discovered in the direction of the open cluster M35 (Williams et al., 2006). We do not yet know whether this object has a proper motion consistent with cluster membership, but this measurement will be revealing. If the hot DQ is, in fact, a cluster member, then because the cluster is only ~ 150 Myr old, if it is a merger, we know that the merger happened on a relatively short time scale. Furthermore, only the most massive stars in the cluster ($\gtrsim 4 M_{\odot}$) have become white dwarfs, which under normal evolution would themselves be quite massive. Thus, if LAWDS 28 is a member of this young stellar population, then it resulted from a merger only if the merger happened quickly and expelled significant mass from the system either during a common envelope or the merger itself. While this may be possible, on the hypothesis that LAWDS 28 formed via a double degenerate merger, we predict it is not a member of the cluster.

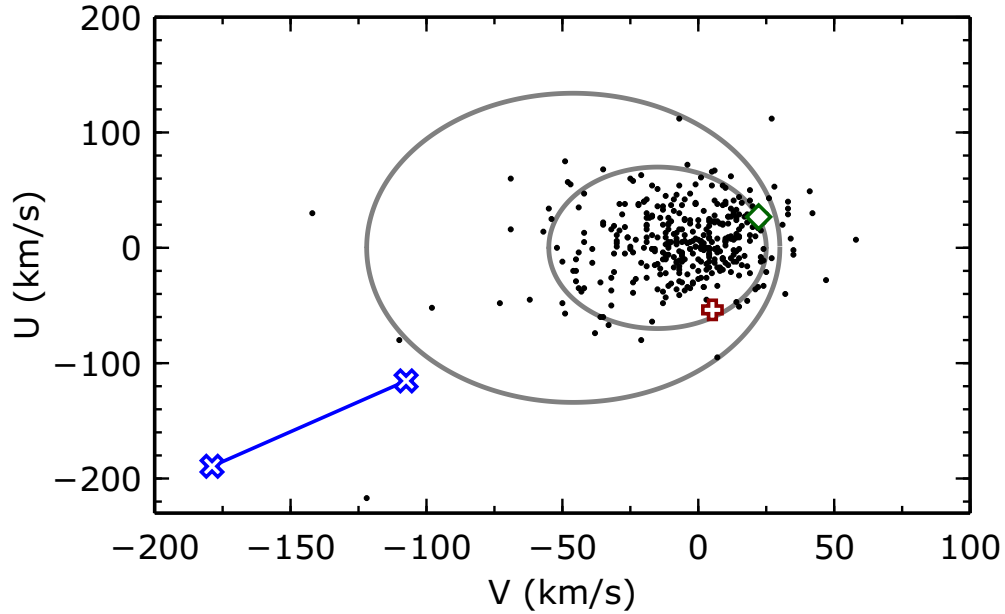


Figure 3.6: Comparison of the Galactic U and V velocity components of the two hot DQs with well-determined distances and SDSS J1153+0056, whose velocity is notable regardless of distance, to a large sample of white dwarfs (black dots) with published kinematics (Farihi et al., 2005). The radial velocities of all stars are set to 0 since they are unknown. The inner/outer ellipses are the bounds containing $\sim 95\%$ of thin/thick disk stars. SDSS J1153+0056 (blue Xs) has a velocity greater than most white dwarfs in the sample whether it is assumed to have $\log g = 8.5$ (lower left X) or $\log g = 9$ (upper right X). SDSS J0005–1002 (red +) is on the outskirts of the central distribution, like older thin disk stars; changes in assumed radial velocity do not change its U velocity appreciably. SDSS J2200–0741 (green diamond) can be moved near the center of the distribution by a $\sim 50 \text{ km s}^{-1}$ change in radial velocity, but this results in its velocity out of the galactic plane (W) being on the tail of that distribution. The velocity errors resulting from the distance uncertainty of SDSS J0005–1002 and SDSS J2200–0741 are smaller than their symbols.

3.3.1 Hot DQs as Double Degenerate Merger Remnants

The old kinematic age of the hot DQ population is the most convincing signature yet that these stars are reheated merger products. It adds to the mounting evidence from photometry and spectroscopy, which we now review, starting with their most apparent peculiarity, their atmospheric composition. White dwarfs typically have atmospheres dominated by hydrogen or helium. The 14 known hot DQs, however, are odd in that their atmospheres are dominated by carbon and oxygen. These elements are expected to be the dominant internal constituents of a white dwarf, but because of the compact object's high surface gravity (10^8 cm s^{-2}), lighter elements rapidly float to the surface and obscure the C/O core. Models with He-layer thicknesses expected from single-star evolution cannot produce hot DQs (Althaus et al., 2009; Koester et al., 2014); however, a merger of two C/O-core white dwarfs may burn the lighter surface elements (Raskin et al., 2012), leaving only a thin layer into which carbon and oxygen could be more easily mixed by convection.

Further evidence for the merger origin of the hot DQs comes from photometry. We saw in chapter 2 that of the 13 hot DQs uncovered by the SDSS, 6 show monoprotic photometric variability. While pulsation has been proposed as an explanation of this variability, their pulse shapes are unlike known white dwarf pulsators, and nearly all white dwarf pulsators are multiprotic with non-harmonically related periods (Fontaine & Brassard, 2008b). We have argued that a better explanation is the rotation of a star with spots. This would require high rotation rates (5 to 20 min) for most of the variables, as expected in mergers where a large reserve of orbital angular momentum can be incorporated into the remnant. The existence of spots requires a magnetic field, which the hot DQs have in much greater abundance than the

general white dwarf population (Dufour et al., 2013). Interestingly, merger models predict that dynamos generate magnetic fields from the circulation of ionized plasma (García-Berro et al., 2012; Ji et al., 2013), and our results provide the first compelling observational evidence that this occurs in actual white dwarf mergers.

In the context of a magnetized, rotating, double degenerate merger remnant, we can ask new questions of the photometric variations. Given that a large store of orbital angular momentum is available to spin up the remnant white dwarf, are the observed photometric periods consistent with expectations for the rotational rates of a merger remnant? We may reasonably expect a merger remnant to be rotating near its break up velocity. Following §7.4 of Shapiro & Teukolsky (1983), we find the maximum angular speed by equating the speed at the equator with the escape speed, $(GM/R)^{1/2}$. For a $1.2 M_{\odot}$ white dwarf, this results in a minimum rotational period of ~ 4 s. A $0.9 M_{\odot}$ white dwarf has a minimum period around twice as large. Furthermore, because such rapidly spinning objects will bulge at the equator, the minimum period may be larger by a factor of 1.8 (Shapiro & Teukolsky, 1983). If SDSS J2200–0741 were spinning close to its break up velocity (~ 15 s) shortly after merging, it would have an angular momentum more than 40 times greater than that suggested by its present photometric period (654 s), and SDSS J0005–1002 has several thousand times less angular momentum than if it were rotating near breakup. Thus, if they originated in mergers, there must be a mechanism to slow them down.

One process, proposed as an effective braking mechanism by García-Berro et al. (2012), is magnetodipole radiation. Their equation 2 shows that $\dot{\Omega} \propto \Omega^3$, where Ω is the angular frequency. Integrating this equation, we find the time it takes to spin down to a given rotation rate:

$$t_{\text{mdr}} = \frac{3Ic^3}{4B^2R^6 \sin^2 \alpha} \left(\frac{1}{\Omega^2} - \frac{1}{\Omega_0^2} \right),$$

where B is the dipolar magnetic field strength, α is the angle between the rotation and magnetic axes, R is the white dwarf radius, Ω_0 is the initial angular frequency, and I is the moment of inertia, which we compute from equation 10 of Külebi et al. (2013). Inserting values appropriate for SDSS J2200–0741 (and letting $B = 5$ MG since the dipolar field strength will be greater than the surface averaged strength), we find $t_{\text{mdr}} = 463$ Gyr to spin down to the currently observed period, assuming the magnetic and rotation axes are orthogonal for maximum braking. Thus, magnetodipole radiation is clearly insufficient to slow a rapidly spinning merger product to the periods observed in hot DQs.

Simulations of double degenerate mergers show that disks are formed around the central remnant, which can receive angular momentum from the white dwarfs via magnetic fields. Külebi et al. (2013) explore these interactions between the central remnant and the disk and find that torques exerted by the disk and winds ejecting particles from the system can slow the rotation of magnetic white dwarfs significantly. In their simulations, a white dwarf with a dipolar field strength of 40 MG can spin down to periods comparable to the short-period hot DQ variables. However, their models with smaller field strengths in the range of the hot DQs continue to rotate at periods on the order of 10s of seconds. It may be that the solution lies in the details of the field generation during the merger. It might be the case, for example, that stronger, short-lived fields are generated, which facilitate magnetic braking before diffusing away from the surface. More detailed numerical simulations are clearly warranted.

In summary, the identification of the hot DQs as merger remnants cleanly resolves the contradiction between their cooling ages and kinematics while naturally accounting for their

peculiar atmospheres, high masses, observed variability, and magnetic fields. As the heretofore missing high-mass white dwarf merger remnants, these stars represent a class of failed type Ia supernovae and provide a well-defined end point against which to test the output of numerical merger simulations. In particular, their mass distribution will test simulations that suggest that conditions for explosion are mass-dependent (Zhu et al., 2013), and their magnetic field strengths will test simulated field generation (García-Berro et al., 2012; Ji et al., 2013). During a merger, magnetic fields would provide a means of transferring energy to the remnant core, which may be a crucial ingredient affecting whether simulated sub-Chandrasekhar mergers become hot enough to ignite carbon (Zhu, 2014).

The hot DQ birthrate may yield yet more important information. The double white dwarf merger rate determined from observations of white dwarf binaries currently has a large uncertainty (Badenes & Maoz, 2012), and the hot DQ space density is similarly uncertain. However, the hot DQ birthrate appears to be roughly 20% to 50% of the white dwarf merger rate. Once both of these rates are better determined, the hot DQ birthrate will place an important constraint on the double degenerate progenitor scenario for type Ia supernovae since the number of mergers that are plausible progenitor candidates must exclude the fraction that produce the hot DQs. We will explore these issues in more detail in the next chapter.

CHAPTER 4: STELLAR ARITHMETIC

“Then how many are there?”

“How many? I don’t know.”

“Quite so! You have not observed. And yet you have seen. That is just my point.”

—An exchange between Holmes and Watson

We have discovered that the masses, motions and brightness fluctuations of the hot DQs are important and revealing properties of the objects. Aside from claiming that each hot DQ is now one where once there were two white dwarfs, we have not considered their number, but it is an important property of the class to examine as we survey how these white dwarf merger remnants fit into a broader astrophysical context.

4.1 Cardinality as an Important Physical Property

Suppose someone suggested a novel way to generate type Ia supernova explosions, perhaps via the head-on collision of two white dwarf stars. Not an inspiraling merger of a double white dwarf binary, but two white dwarfs actually running headlong into one another after having been set upon that collision course by a third star orbiting around the inner white dwarf binary system and perturbing the inner orbit with its gravitational tug. You might initially be incredulous that this could be the recipe to make a typical type Ia supernova. If so, that incredulity is likely not based on your physical intuition that the nuclear cooking of the heavy elements in an explosion prepared in such a way would fail to produce the amounts of nickel, iron, etc. typical of a type Ia supernova. Rather, the initial suspicion likely arises from a sense

that the ingredients are too rare. How often, after all, will a pair of white dwarfs find themselves in such a hierarchical triple system, and among those, how many will collide because of the perturbing effects of a third body? And won't this surely happen far less often than type Ia supernovae?

Exactly such a scenario has recently been proposed (Kushnir et al., 2013), and just such objections have been anticipated (Katz & Dong, 2012; Katz et al., 2014) and mooted (Naoz & Fabrycky, 2014). We raise this here not to offer an opinion about this particular progenitor model but to emphasize that besides the many observed features of type Ia supernovae explosions that models of them must reproduce, the model progenitor systems must also be reflected in nature in sufficient numbers to account for the number of type Ia supernovae.

In recent years both of the primary type Ia progenitor scenarios (single-degenerate and double-degenerate) have run up against the problem that there do not appear to be enough of them to produce the observed type Ia supernova rate. We will review these issues and also look at how the hot DQs fit into the picture and how they fare in the numbers game. We have shown that the best explanation for the known properties of the hot DQs is that they come about through double degenerates that merge without exploding. We will consider whether there are enough known double degenerate systems to explain the number of hot DQs, and because their possible progenitors overlap with a subset of potential type Ia supernova progenitors in the double-degenerate scenario, our result will then provide information crucial to determining whether there are enough such systems that might explode upon coalescing.

We begin with a review of how the two primary progenitors scenarios fare in terms of being able to account for the number of type Ia supernovae. (See Maoz et al. (2014) for a recent general overview of the progenitor problem.) As a reference, we will need to know the

observed rate of type Ia supernovae. For galaxies like our own (Sbc spirals), Li et al. (2011) find that type Ia supernovae occur at a rate of $1.1 \times 10^{-13} \text{ yr}^{-1} M_{\odot}^{-1}$ (where the mass refers to stellar mass). For a Milky Way mass of $6.4 \times 10^{10} M_{\odot}$ (McMillan, 2011), this translates into an average of one SN Ia every ~ 150 years.¹ And, given a stellar density in the solar neighborhood of $0.087 M_{\odot} \text{ pc}^{-3}$ (McMillan, 2011), the local SN Ia rate per unit volume is $9.6 \times 10^{-15} \text{ yr}^{-1} \text{ pc}^{-3}$. Since the hot DQs and observed samples of double degenerate merger candidates all lie within a few hundred parsecs, this local rate is the appropriate number for comparison.

4.2 The Single Degenerate Scenario

The textbook single degenerate model for the creation of a type Ia supernova pushes the white dwarf to a mass near the Chandrasekhar limit ($\sim 1.4 M_{\odot}$, the mass limit above which a white dwarf will collapse, Chandrasekhar, 1931; Hamada & Salpeter, 1961) where its central density becomes high enough to begin fusing carbon. The presentation of this classic scenario for a type Ia supernova (Whelan & Iben, 1973) optimistically assumes that many stars will embark upon their lives as white dwarfs with masses much closer to the Chandrasekhar mass than is actually the case. Later observations (Koester et al., 1979; Weidemann & Koester, 1984) show that mass loss conspires to yield a very narrow white dwarf mass distribution centered on $0.6 M_{\odot}$ with a very small fraction extending towards the $\sim 1.38 M_{\odot}$ needed to explode the star (Fig. 3.1). Furthermore, the most massive white dwarfs ($M \gtrsim 1.1 M_{\odot}$) are thought to have been massive enough to proceed past helium fusion on to carbon burning, which will produce an oxygen/neon core (García-Berro et al., 1997; Gil-Pons et al., 2003) rather than the carbon/oxygen

¹See Li et al. (2011) for a discussion of the systematic rate uncertainties, which may be roughly a factor of 2 for the Milky Way.

core necessary for type Ia supernovae.² Thus, any single degenerate progenitor candidate will have to accumulate at least $\sim 0.3 M_{\odot}$ of material from a companion before a possible explosion, and the typical less-massive white dwarf will have to accrete much more. This means the number of possible single-degenerate progenitor systems is significantly diminished compared to the assumptions about available systems when it was originally proposed.

This is, of course, not a problem for the single-degenerate progenitor scenario if there are still plausibly enough systems to explain the Ia supernova rate. This, however, does not seem to be the case. Theoretical population synthesis studies by Ruiter et al. (2009) find that the number of white dwarfs that will accumulate a sufficient amount of mass from a non-degenerate companion star to explode as a near-Chandrasekhar mass type Ia supernova is far below the observed number of explosions. For a Milky Way-like galaxy, they find a rate that is more than a factor of 10 below the observed rate.

The number of single-degenerate systems where the white dwarf is the recipient of a stable flow of matter from a non-degenerate companion is plausibly larger than the number of type Ia supernovae. The problem, however, is that this is only a necessary and not a sufficient condition to effect an explosion. The white dwarf not only has to acquire matter from its donor star, it must also retain it, but in some model systems, this depends sensitively on how quickly the mass is transferred (Fujimoto, 1982; Nomoto et al., 2007). If the transfer rate is too low, the new material accumulated on its surface will become sufficiently hot at its base that the matter detonates in an explosion observed as a classical nova. This explosive event may be energetic enough to eject a significant amount of the matter gained from the companion (Yaron et al.,

²Because they release a significant amount of their nuclear energy fusing carbon to neon as super AGB stars, O/Ne-core white dwarfs would not release sufficient energy in a thermonuclear explosion to produce a typical type Ia SNe.

2005). These systems will never grow in mass enough to compress the core to the point of triggering a supernova explosion.

If, on the other hand, the rate of mass transfer is too high, the luminosity of the white dwarf becomes so high that its radiation pressure ejects mass from the system (Nomoto et al., 2007). The necessary conditions for a type Ia supernova from a single-degenerate progenitor, therefore, include the following: 1) a white dwarf with a C/O core, so a mass between ~ 0.45 and $1.1 M_{\odot}$; 2) a companion star sufficiently massive that it can contribute enough mass to the white dwarf to push it to the Chandrasekhar mass, so at least $0.3 M_{\odot}$ for companions to the most massive accretors; 3) a mass transfer rate that is not too high or too low but just right so the white dwarf can grow in mass.

Such systems appear to exist, but Ruiter et al. (2009) find that there are not enough to account for the observed type Ia supernova rate in their synthetic binary populations. Because they are continually releasing a large amount of energy from the accreting hydrogen that is burning on their surfaces, the systems that are tuned to grow in mass are expected to become supersoft X-ray sources (Hachisu et al., 1999), which allows an observational inquiry into the number of possible single-degenerate progenitors. The observed X-ray luminosities of elliptical galaxies are far below the luminosities expected from the number of single-degenerate progenitors necessary to produce type Ia supernova rates typical for these galaxies, and the discrepancy is not small: single-degenerate progenitors manifesting as supersoft sources can only account for 5% of the type Ia rate in these stellar populations (Gilfanov & Bogdán, 2010).

However, the identification of supersoft sources as progenitors depends on model-dependent assumptions about the conditions on the surface of a white dwarf accreting matter at the just-right accretion rates that lead to mass growth. In particular, the conclusion that these systems

will be supersoft X-ray sources follows from the assumption that white dwarfs with these accretion rates will undergo steady nuclear burning, i.e., that they will fuse the hydrogen at the same rate it is arriving on the surface (Gilfanov & Bogdán, 2010). Numerical simulations using the best nuclear reaction rates, however, do not find steady burning. They instead see periodic fusion events, and unlike the novae explosions resulting from slower accretion rates, these simulated fusion events do not remove matter from the white dwarf but instead result in mass growth over time (Hillman et al., 2015; Starrfield et al., 2012a,b). The implication is that many possible single-degenerate type Ia supernova progenitors may not manifest as supersoft sources, so the observed number of these may not be as problematic for the single-degenerate scenario as it seems given the assumption of steady burning.

In the current simulations of accretion-induced nuclear burning on a white dwarf's surface, a condition for avoiding the explosive removal of mass from the surface is that C/O core material is not mixed with the accreted material. The presence of core-material results in simulated nova explosions energetic enough to remove much of the mass accreted since the previous thermonuclear event (Starrfield et al., 2012a). It is not clear whether this no-core-material condition is likely to be met in actual accreting white dwarfs. In at least one case, the ejecta from a recurrent nova (T Pyxidis) has been observed to have significant amounts of oxygen, suggesting the accreted material was mixed with core material (Chomiuk et al., 2014). On the other hand, observations show that white dwarfs in accreting systems have a mass distribution shifted towards higher mass than white dwarfs in post-common-envelope binaries, which are presumed to be the progenitors of these accreting systems (Zorotovic et al., 2011). A straightforward explanation of this is that the white dwarfs grow in mass. The recurrent nova RS Ophiuchi stands as an example of an accreting white dwarf near the Chandrasekhar mass

that appears to be growing in mass and poised to explode as a type Ia supernova (Sokoloski et al., 2006).

Determining the number of potential single-degenerate progenitors of type Ia supernovae is clearly complicated, and the answer is unsettled. Yet several observations of nearby type Ia supernovae also present considerable challenges to the single degenerate scenario. These include the absence of hydrogen signatures in the circumstellar environment and only a small fraction showing circumstellar material at all (which would be expected for a system undergoing mass transfer) and no confirmed secondaries in pre- or post-imaging data. (Again, see Maoz et al. (2014) for a comprehensive review of the progenitor situation and Kasen & Nugent (2013) for the implications of a well-studied nearby Ia SNe). The potential significant shortfall in the number of single-degenerate progenitors combined with observations such as these has prompted renewed interest in the double-degenerate progenitor scenario (van Kerkwijk, 2013).

4.3 The Double Degenerate Scenario

The classical double degenerate scenario involves the merger of two white dwarfs with a total mass greater than the Chandrasekhar mass (Iben & Tutukov, 1984; Webbink, 1984). These systems appear to fare better in explaining the observed supernova rate than the single degenerate scenario, but their number still falls short (Ruiter et al., 2009). Motivated by the possible paucity of classical progenitor systems, van Kerkwijk et al. (2010) propose that the constraint that type Ia supernovae result from the explosion of white dwarfs near the Chandrasekhar mass might not be necessary. Masses near the Chandrasekhar limit are often invoked as a necessary ingredient for producing an explosion. In these scenarios, the central densities of the degenerate material rise to the point where pycnonuclear reactions instigate the supernova. However, if the central temperature were high enough, an explosion could occur at

much lower densities and thus lower mass. Van Kerkwijk et al. propose a scenario in which the effect of the violent merger of two white dwarfs is to heat the core to temperatures high enough that this takes place. This removes high mass as a necessary condition of a type Ia supernova and so expands the number of possible progenitors.

However, the question then arises whether systems with a range of sub-Chandrasekhar masses can produce the ^{56}Ni necessary to power observed type Ia SNe. Piro et al. (2014) show that this is plausible if the mass of the exploding remnant is roughly equal to the total mass of the merging system rather than the mass of the primary. Such complete mergers are found in simulations where the merging white dwarfs are roughly equal in mass (Zhu, 2014).

Van Kerkwijk et al. point out that the total merger rate of double C/O-core white dwarf stars is high enough to account for the type Ia supernova rate. Their calculation of the white dwarf merger rate is an analytic determination based on the output of various simulations, but thanks to the SDSS, there are also observational constraints on this rate.

4.3.1 The Double Degenerate Merger Rate

Empirically, the best estimate of the white dwarf merger rate in our galaxy comes from SDSS spectra of white dwarfs taken at multiple epochs (Badenes & Maoz, 2012). If the white dwarfs are in binaries with other white dwarfs, typically only one of the components is visible in the spectrum, but its spectral lines will shift back and forth because of its orbital motion, and the amplitude of these observed radial velocity variations depends on the orbital separation and white dwarf masses. The observed distribution of maximum radial velocity shifts between epochs in the SDSS data directly constrains the binary fraction and distribution of separation distances of the binary components. Then, under assumptions about the primary and secondary

white dwarf mass distributions, the white dwarf merger rate of the population can be calculated³ (Maoz et al., 2012).

Using this method, Badenes & Maoz (2012) constrain the super-Chandrasekhar merger rate to 0.1×10^{-13} mergers $\text{yr}^{-1} M_{\odot}^{-1}$ (with a 95% confidence interval from 0.016 to 0.4 in the same units). In agreement with population synthesis studies, this falls well short of the type Ia rate. They find the total WD merger rate, on the other hand, to be 1.4×10^{-13} mergers $\text{yr}^{-1} M_{\odot}^{-1}$ (with a 95% confidence interval from 0.16 to 7.2). Though the uncertainty is large, the best-fit value is extremely close to the type Ia supernova rate (Cf. the rate of rate of $1.1 \times 10^{-13} \text{ yr}^{-1} M_{\odot}^{-1}$ from Li et al. 2011). This lends support to the argument of van Kerkwijk et al. (2010) that violent white dwarf mergers with a total mass below the Chandrasekhar limit may account for typical type Ia supernovae.

However, to know whether double degenerate mergers can account for all or even some fraction of type Ia supernovae, the crucial rate to determine is ultimately not the white dwarf merger rate but that rate minus the rate of white dwarf mergers known to have non-explosive fates. Since we think that the hot DQs constitute these remnants, the next step is to compute their formation rate so that it can be compared to the Badenes & Maoz (2012) WD+WD merger rate.

4.4 How Many Hot DQs Are There?

The first step in answering this question is to determine the hot DQ space density. Then, given the time it takes them to cool through the temperature range over which we observe them, we will know their formation rate per unit volume. We face two difficulties in computing their

³The results depend only weakly on the assumptions about secondary mass, which can be uncertain because of uncertainties in models of common envelope evolution leading to varying amounts of mass loss.

space densities. As we have seen before, we do not know the distances to most of the hot DQs, and these are crucial for knowing their space density. The second confounding factor is that we do not know what fraction of hot DQs present in the SDSS spectroscopic area that the survey missed. However, we will make reasonable assumptions about both of these, and proceed to compute hot DQ space densities, keeping in mind these important sources of uncertainty.

Fortunately, several of the hot DQs are flagged with the `hot_standard` flag based on their color (both $u - g$ and $g - r < 0$) and magnitude ($g < 19$). These targets were given high priority in the survey and therefore have a relatively high completeness (Blanton et al., 2003; Krzesinski et al., 2009). Krzesinski et al. (2009) exploit this to construct a luminosity function for hot white dwarf stars, and they also provide a completeness map across the DR4 survey area for `hot_standard` objects in various ranges of magnitude. Typical completeness factors are around 70%, so we adopt this relatively high completeness in our space density calculations.

Besides corrections for targeting completeness, we also correct for the magnitude limits of the survey using the $1/V_{\max}$ method described in Schmidt (1968) and frequently employed in computing white dwarf space densities (e.g., De Gennaro et al. 2008; Liebert et al. 2005). This method accounts for missing bright and faint objects from the survey's saturation and faint magnitude limits. The final correction we employ also attempts to account for the exponential vertical drop off in the density of stellar populations moving out from the midplane of the Galaxy. We assume the density is proportional to e^{-z/z_0} , and we set the scaleheight, z_0 , to 250 pc, which is consistent with that used in previous determinations of white dwarf space densities. For each star, we compute

$$V_{\max} = \frac{4\pi}{3}\beta(r_{\max}^3 - r_{\min}^3)e^{-z/z_0},$$

and we take r_{\max} to be the distance at which the star would have an apparent magnitude of

$g = 19$ and r_{\min} to be the distance at which it would have the magnitude $g = 15$. The spectroscopic area in DR7 of the SDSS covers a fraction of the sky, $\beta = 0.23038$. The space density is then given by the sum of the $1/V_{\max}$ values for all stars in the sample. For the hot DQs without parallaxes, we use the distances determined from assuming $\log g = 8.5$ as in chapter 3.

The hot DQ sample includes 10 stars down to $g = 19.0$. Using these and assuming the DR7 spectroscopic targeting missed 30% of the hot DQs in the survey area, we determine a space density of $7.35 \times 10^{-7} \text{ pc}^{-3}$. If we limit our selection to those hot DQ stars that are actually flagged in the SDSS photometry as hot_standard stars, the sample is reduced to 8 stars, and the resulting space density is $6.63 \times 10^{-7} \text{ pc}^{-3}$, again assuming a 70% completeness. In the discussion below, we adopt a value of 7×10^{-7} hot DQs per pc^3 . The uncertainty of this value is 30% from the small number statistics, and somewhat higher due to the uncertain survey completeness. Assuming a mass closer to $1.2 M_{\odot}$ increase the space density by roughly a factor of 2.

4.4.1 The Hot DQ Formation Rate

The observed hot DQs have temperatures that fall roughly in the range 19,000–25,000 K. A model star with a helium atmosphere at our assumed mass ($\approx 0.9 M_{\odot}$) takes 137 Myr to cool across this range (Fontaine et al., 2001). Under these assumptions, the hot DQ formation rate is $5.1 \times 10^{-15} \text{ yr}^{-1} \text{ pc}^{-3}$. We note that if the hot DQs are, on average, more massive than what we are assuming here (which is likely for C/O-core mergers), then their distances are closer than what we are assuming, so their space density will increase. However, because their radiating surface area also decreases with increased mass, the time it takes them to cool across the observed temperature range increases, and the two effects roughly cancel so that the formation rate is less subject to the uncertainty in mass than the space density.

The WD+WD merger rate from Badenes & Maoz (2012) (§ 4.3.1) is 1.4×10^{-13} mergers $\text{yr}^{-1} M_{\odot}^{-1}$. Using the local stellar density of $0.087 M_{\odot} \text{pc}^{-3}$ (McMillan, 2011), this translates to 1.2×10^{-14} mergers $\text{yr}^{-1} \text{pc}^{-3}$. This is a little more than twice as large as the hot DQ formation rate we just derived. However, this rate from Badenes & Maoz (2012) is the rate for all WD+WD mergers, regardless of mass. Those above the Chandrasekhar mass will explode or possibly collapse to form neutron stars, and those with relatively low total masses, are either the result of two He-core white dwarfs merging or the result of a He-core and a C/O-core white dwarf merger. We should thus like to narrow our inquiry to those mergers that might represent two C/O-core white dwarfs since these are the most plausible progenitor candidates for the carbon/oxygen atmosphere hot DQs.

The derived rate of double C/O-core white dwarf mergers is not explicitly given in Badenes & Maoz (2012); however, they do provide the total merger rate, the super-Chandrasekhar rate, and, in Maoz et al. (2012), the merger rate with total mass $< 1 M_{\odot}$. These values imply a merger rate of $6.4 \times 10^{-15} \text{yr}^{-1} \text{pc}^{-3}$ for total mass between $1 M_{\odot}$ and the Chandrasekhar mass. It is therefore possible that the hot DQ formation rate is a significant fraction of the C/O-core white dwarf merger rate found by Badenes & Maoz. However, within their 95% confidence interval, their total merger rate can be a factor of 5 larger than the best-fit value (the 1σ value can be more than a factor of 3 larger); their double C/O white dwarf merger rate is likely equally uncertain. This, combined with the uncertainties in our determination of the hot DQ birthrate do not permit strong conclusions at this point.

Nonetheless, the double degenerate scenario for the origin of the hot DQs passes an important test. There are plausibly enough WD+WD merger candidates observed in the SDSS of sufficient total mass to account for the number of hot DQs we observe. Furthermore, though

the hot DQs may represent a significant fraction of the candidate sub-Chandrasekhar mergers, there appear to be enough candidates within the 1σ range of the Badenes & Maoz (2012) double C/O white dwarf merger rate to account for hot DQ formation with enough systems left over to explode as type Ia supernovae. Better determinations of both rates are clearly important.

4.5 Where Do The Hot DQs Go?

Having provided an answer to the question of their origin, it is also worthwhile to ask where the hot DQs go once they have cooled beyond the hot DQ phase. It is plausible that whatever helium they have in their atmospheres will once again make its way to the top of the carbon and oxygen so that the carbon-dominated atmospheres will become helium-dominated but with detectable amounts of carbon enrichment. Dufour et al. (2013) have suggested that the hot DQs thus form a continuous sequence with the “warm” DQs that show C I lines and then eventually cool to become the second sequence of cool DQs, a distinct higher carbon-abundance sequence of cool DQs in the $[C/He]$, T_{eff} plane (Dufour et al., 2005; Koester & Knist, 2006).

Since cooler white dwarfs cool more slowly than hotter white dwarfs, we expect to find more hot DQ progeny in a given volume than hot DQs. To calculate the number expected in a spherical volume with radius R , we must integrate the space density over that volume. Because the stellar density varies exponentially from the Galactic midplane, the result is not simply the product of the density and the spherical volume in question but is instead given by

$$N(R) = 2\pi\rho_0(2z_0Re^{-R/z_0} + R^2h_0 + 2h_0^3(e^{-R/z_0} - 1)).$$

We use $z_0 = 250$ pc to be consistent with our above determination of space density.

The population of warm DQs discussed in Dufour et al. (2013) lies roughly in the temperature range 18,000–12,000 K. Cooling through this range takes model $0.9 M_{\odot}$ white dwarfs 540 Myr, which is 4 times longer than it takes the stars to pass through the hot DQ phase. The

descendants of the hot DQs in this temperature range should therefore have a factor of 4 higher space density, so $\rho_0 = 2.8 \times 10^{-6} \text{ pc}^{-3}$. Down to a magnitude limit of $g \sim 19$, we expect to see these stars out to $R = 200 \text{ pc}$. Using the above equation, we therefore expect 70 warm DQs within 200 pc (210 within 300 pc). Assuming the sample is more massive, these values could be higher by a factor of ~ 2 because of the increased cooling time through the range. These numbers will be useful in comparing to the number of warm DQs in forthcoming samples uncovered by the SDSS.

We also expect that the cooler descendants of hot DQs will be massive and that they will have kinematics that distinguish them from a population of singly-evolved white dwarfs of the same mass and temperature. Already, there is growing evidence that the warm DQ white dwarfs tend to be massive. Those with parallax measurements (G35–26, G227–5, G47–18, and SDSS J1328+59) indicate their masses are greater than the Sun’s. Furthermore, the current best-fit spectroscopic model of the variable warm DQ SDSS J1036+6522 discussed in § 2.4.3 suggests it is massive (Williams et al., 2013). As white dwarfs become cooler, it becomes increasingly difficult to determine whether their kinematics are distinctly older than their single-star ages because their white dwarf cooling ages become long and uncertainties in cooling physics mean the cooling ages have large uncertainties. Nonetheless, the kinematics should be revealing, especially for the recently discovered large population of warm DQs (Dufour et al., 2013). We note that one of the first investigations to look for kinematic differences among white dwarf spectral classes found the cool DQs to have distinctly larger space motions than other spectral types (Sion et al., 1988). If the cool DQs contain a significant population of massive stars, then the assumption of typical white dwarf masses as in Sion et al. (1988) will lead to artificially large velocities (because of the distance overestimates). This may account in part

for their findings; nonetheless, the apparently distinct cool DQ kinematics of Sion et al. were a harbinger of the results shown in chapter 3.

In this vein, we call attention to LP 93–23 (a.k.a., LHS 291, a DQ classified in the SDSS DR7 white dwarf catalog as having C I lines), which in retrospect provided perhaps the first evidence that the DQs harbored a population of white dwarfs with kinematic ages older than expected from single-star evolution. In 1968, Luyten (IAU Circular No. 2069) discovered that it had an extreme proper motion, and this was followed-up immediately by Sandage (Ibid.), who acquired photoelectric photometry of the object using the Hale reflector. Sandage discussed its extreme velocity and also highly eccentric and even retrograde Galactic orbit. Because of its large velocity, it has been discussed as a candidate member of the galactic halo, yet because it was initially thought to have a cool temperature (~ 4000 K; Sion et al. 1988), its status as a member of an old stellar population seemed consistent with a very long cooling age as a white dwarf, which might also be of typical mass and so have had a long main-sequence lifetime. However, its SDSS spectrum reveals the presence of C I lines, suggesting it is relatively warm and, so, has a cooling age no more than 2.5 Gyr (for the most massive models, and shorter cooling times for less-massive models).

Weidemann (2005) provides an updated Yale parallax and also infers a warm temperature from its colors ($\sim 8,000$ – $9,000$ K). With a proper motion of 1.77 arcsec yr⁻¹, the parallax quoted in Weidemann (2005) implies a velocity of 800 km s⁻¹ (530 – 1630 km s⁻¹ given the 1σ parallax error). Weidemann argues for a high-mass for LP 93–23, consistent with the parallax. Even at the best-fit value of the parallax, the star is $0.7 M_{\odot}$, in which case it had a sufficiently short main-sequence lifetime that its total age is far too young to explain its halo-like velocity and Galactic orbit. LP 93–23 seems to be just the sort of hot DQ descendant we would expect to

find. However, if a more precise parallax measurement shows its velocity to be on the high end of the currently permitted range, LP 93–23 would have an uncomfortably peculiar motion difficult to explain via typical disk heating.

4.6 Future Research Directions and Further Implications

We close by hinting at possible research directions and also gesturing towards some other interesting implications of the hot DQs as double degenerate mergers. We have already pointed out some work that needs to be done, including a better determination of the hot DQ space density along with a better determination of the double degenerate merger rate. The former depends on finding more hot DQs and also determining parallaxes for more, which is also necessary for determining their mass distribution.

In chapter 2, we also saw the importance of long-term photometric monitoring of all the hot DQs to discover possible long-term variability resulting from the rotation of magnetic spots. The population of warm DQs should also be monitored for long and short-period photometric variability, and their kinematics should be analyzed. Concerning kinematics, it is also important to decrease the errors on the transverse velocity distribution from chapter 3. To that end, we are obtaining a new epoch of position measurements for all of the hot DQs available to SOAR, which we can combine with the SDSS imaging, most of which was taken more than 10 years ago, to determine more precise proper motions.

In the following sections, we draw attention to other potentially interesting work related to the hot DQs.

4.6.1 Planets

The hot DQs are relevant to exoplanet research in two ways. The detection of planetary systems around massive white dwarfs is an important probe of the incidence of planetary

systems around massive main-sequence stars, which are themselves less amenable than lower-mass main-sequence stars to planetary detection (Barber et al., 2014, 2012). A primary method of searching for such remnant planetary systems around white dwarfs is the detection of infrared excess. However, since massive white dwarfs can also come from mergers and since mergers may produce a disk of remnant material that could cool and manifest as an infrared excess, mergers are a possible contaminant for this method (Hansen et al., 2006; Livio et al., 2005). If the hot DQs can be established as constituting most or all massive white dwarf merger remnants, then inferences about planetary systems around massive single-star progenitors will be on a secure footing. Second, possible debris forming a disk in a WD+WD merger might provide the material for forming planets of atypical C/O composition (Livio et al., 2005). The hot DQs thus become interesting candidates for planet searches. Conveniently their periodic brightness variations can be used to detect orbital motion (Barlow et al., 2011; Mullally et al., 2008).

4.6.2 Galactic Merger History

In principal, the luminosity function, masses, and kinematics of the hot DQs and their descendants allow these remnants of white dwarf mergers to be used to reconstruct the double degenerate merger history of the Galaxy in the same way that the white dwarf remnants of single-star evolution can be used to reconstruct the star formation history of the Galaxy (Rowell, 2013; Tremblay et al., 2014; Winget et al., 1987). The parallaxes and proper motions provided by the Gaia mission (Jordan, 2014) will be an important step in this direction.

4.6.3 Theory

Because a C/O-core white dwarf's He-layer is extremely small compared to the rest of the star, these layers are often ignored in merger simulations (but see Raskin et al. (2012)

and Pakmor et al. (2013)). However, carefully following the evolution and nuclear burning of the helium during such simulations is important in determining whether simulated mergers can reproduce the thin He-layers that are required for the convective mixing scenario for the transition of a He-atmosphere white dwarf to a hot DQ. A related theoretical task is to take the output of such a merger simulation and let it cool to hot DQ temperatures with a stellar evolution code such as MESA (Paxton et al., 2013) to see if a hot DQ comes about naturally given this initial structure, which will clearly be very different from the model outputs of a star emerging from the AGB phase.

4.7 Summary and Conclusion

Our contention that the hot DQs are merger remnants may, of course, turn out to be wrong. Nonetheless, there is value in pushing a concept and drawing out its natural consequences to see how it fits with and informs other areas of our knowledge. In chapter 2 we have seen that the magnetic rotator explanation for hot DQ variability is naturally able to explain the important features of the brightness variations observed in the DQs and also account for all observed DQ variability with a common cause. In chapter 3 we showed that the motions of the hot DQs imply that they have been circulating through the galaxy much longer than expected from their temperatures and masses. This helps establish the hot DQs as the missing high-mass double degenerate merger products. A direct implication is that that they are the next of kin to type Ia supernovae arising from double degenerate mergers.

Furthermore, the high fraction of magnetism among the hot DQs provides the best observational evidence that the merger of two white dwarfs can create such fields, a phenomenon that has been predicted (García-Berro et al., 2012; Ji et al., 2013) and may also play a crucial role in the detonation of simulated mergers (Zhu, 2014). In this context, the hot DQs become

the observational standards against which to calibrate simulations of cosmological distance standards.

Because they did not explode upon merging, the hot DQs must be accounted for when attempting to determine whether there are enough double degenerate mergers to explain the supernova rate. We have taken a go at this in the present chapter using numbers whose uncertainties are currently rather large, but we see that the numbers are consistent with a merger origin for the hot DQs, and that there could be enough merger systems remaining to account for much of the type Ia supernova rate.

When gravity begins the long process of pulling together a white dwarf out of hydrogen-rich gas, it sometimes goes by an even longer route, first making two white dwarfs and then, slowly, pulling them together till at last there is a violent collision between two objects the size of the Earth and 200,000 times more massive. It is hard to imagine what happens next. Fortunately, we are not left entirely to our imaginations; because of the hot DQs, we get to look and see.

REFERENCES

- Althaus, L. G., Córscico, A. H., Isern, J., & García-Berro, E. 2010, *A&A Rev.*, 18, 471
- Althaus, L. G., García-Berro, E., Córscico, A. H., Miller Bertolami, M. M., & Romero, A. D. 2009, *ApJ*, 693, L23
- Aristotle. 2001, *The Basic Works of Aristotle*, ed. R. McKeon (Modern Library)
- Aumer, M., & Binney, J. J. 2009, *MNRAS*, 397, 1286
- Badenes, C., & Maoz, D. 2012, *ApJ*, 749, L11
- Baldry, I. 1999, PhD thesis, University of Sydney
- Barber, S. D., Kilic, M., Brown, W. R., & Gianninas, A. 2014, *ApJ*, 786, 77
- Barber, S. D., Patterson, A. J., Kilic, M., et al. 2012, *ApJ*, 760, 26
- Barlow, B. N., Dunlap, B. H., & Clemens, J. C. 2011, *ApJ*, 737, L2
- Barlow, B. N., Dunlap, B. H., Rosen, R., & Clemens, J. C. 2008, *ApJ*, 688, L95
- Belopolsky, A. 1894, *Astronomische Nachrichten*, 136, 281
- Bensby, T., Feltzing, S., & Lundström, I. 2003, *A&A*, 410, 527
- Benz, W., Cameron, A. G. W., Press, W. H., & Bowers, R. L. 1990, *ApJ*, 348, 647
- Bergeron, P., Leggett, S. K., & Ruiz, M. T. 2001, *ApJS*, 133, 413
- Bergeron, P., Ruiz, M. T., & Leggett, S. K. 1997, *ApJS*, 108, 339
- Bergeron, P., Wesemael, F., Dufour, P., et al. 2011, *ApJ*, 737, 28
- Blanton, M. R., Lin, H., Lupton, R. H., et al. 2003, *AJ*, 125, 2276
- Brinkworth, C. S., Burleigh, M. R., Lawrie, K., Marsh, T. R., & Knigge, C. 2013, *ApJ*, 773, 47
- Brunt, D. 1913, *The Observatory*, 36, 59
- Chandrasekhar, S. 1931, *ApJ*, 74, 81
- Chomiuk, L., Nelson, T., Mukai, K., et al. 2014, *ApJ*, 788, 130
- Clemens, J. C., Crain, J. A., & Anderson, R. 2004, in Presented at the Society of Photo-Optical Instrumentation Engineers (SPIE) Conference, Vol. 5492, Society of Photo-Optical Instrumentation Engineers (SPIE) Conference Series, ed. A. F. M. Moorwood & M. Iye, 331–340
- Clemens, J. C., Nather, R. E., Winget, D. E., et al. 1992, *ApJ*, 391, 773

- Córsico, A. H., Romero, A. D., Althaus, L. G., & García-Berro, E. 2009, *A&A*, 506, 835
- Cumming, A., Marcy, G. W., & Butler, R. P. 1999, *ApJ*, 526, 890
- Dahn, C. C., Harris, H. C., Vrba, F. J., et al. 2002, *AJ*, 124, 1170
- De Gennaro, S., von Hippel, T., Winget, D. E., et al. 2008, *AJ*, 135, 1
- Degennaro, S., Williams, K., & Montgomery, M. 2008, *Information Bulletin on Variable Stars*, 5900, 9
- Dufour, P. 2011, *Stars with Unusual Compositions: Carbon and Oxygen in Cool White Dwarfs*, ed. D. W. Hoard (Weinheim, Germany: Wiley-VCH), 53–88
- Dufour, P., Béland, S., Fontaine, G., Chayer, P., & Bergeron, P. 2011a, *ApJ*, 733, L19
- Dufour, P., Ben Nessib, N., Sahal-Bréchet, S., & Dimitrijević, M. S. 2011b, *Baltic Astronomy*, 20, 511
- Dufour, P., Bergeron, P., & Fontaine, G. 2005, *ApJ*, 627, 404
- Dufour, P., Fontaine, G., Bergeron, P., et al. 2010, in *American Institute of Physics Conference Series*, Vol. 1273, *American Institute of Physics Conference Series*, ed. K. Werner & T. Rauch, 64–69
- Dufour, P., Fontaine, G., Liebert, J., Schmidt, G. D., & Behara, N. 2008a, *ApJ*, 683, 978
- Dufour, P., Fontaine, G., Liebert, J., Williams, K., & Lai, D. K. 2008b, *ApJ*, 683, L167
- Dufour, P., Green, E. M., Fontaine, G., et al. 2009, *ApJ*, 703, 240
- Dufour, P., Liebert, J., Fontaine, G., & Behara, N. 2007, *Nature*, 450, 522
- Dufour, P., Vornanen, T., Bergeron, P., & Fontaine, A., B. 2013, in *Astronomical Society of the Pacific Conference Series*, Vol. 469, *18th European White Dwarf Workshop.*, ed. Krzesiń, J. ski, G. Stachowski, P. Moskalik, & K. Bajan, 167
- Dunlap, B. H., Barlow, B. N., & Clemens, J. C. 2010, *ApJ*, 720, L159
- Eddington, A. S. 1917, *The Observatory*, 40, 290
- Farihi, J., Becklin, E. E., & Zuckerman, B. 2005, *ApJS*, 161, 394
- Ferrario, L., Wickramasinghe, D., Liebert, J., & Williams, K. A. 2005, *MNRAS*, 361, 1131
- Fontaine, G., & Brassard, P. 2008a, *PASP*, 120, 1043
- . 2008b, *PASP*, 120, 1043
- Fontaine, G., Brassard, P., & Bergeron, P. 2001, *PASP*, 113, 409
- Fontaine, G., Brassard, P., & Dufour, P. 2008, *A&A*, 483, L1

Fujimoto, M. Y. 1982, *ApJ*, 257, 767

García-Berro, E., Ritossa, C., & Iben, Jr., I. 1997, *ApJ*, 485, 765

García-Berro, E., Lorén-Aguilar, P., Aznar-Siguán, G., et al. 2012, *ApJ*, 749, 25

Gil-Pons, P., García-Berro, E., José, J., Hernanz, M., & Truran, J. W. 2003, *A&A*, 407, 1021

Gilfanov, M., & Bogdán, Á. 2010, *Nature*, 463, 924

Girardi, L., Bressan, A., Bertelli, G., & Chiosi, C. 2000, *A&AS*, 141, 371

Goodricke, J. 1786, *Royal Society of London Philosophical Transactions Series I*, 76, 48

Green, E. M., Dufour, P., Fontaine, G., & Brassard, P. 2009, *ApJ*, 702, 1593

Hachisu, I., Kato, M., & Nomoto, K. 1999, *ApJ*, 522, 487

Hamada, T., & Salpeter, E. E. 1961, *ApJ*, 134, 683

Hansen, B. M. S., Kulkarni, S., & Wiktorowicz, S. 2006, *AJ*, 131, 1106

Hillman, Y., Prialnik, D., Kovetz, A., & Shara, M. M. 2015, *MNRAS*, 446, 1924

Holberg, J. B., & Bergeron, P. 2006, *AJ*, 132, 1221

Horne, J. H., & Baliunas, S. L. 1986, *ApJ*, 302, 757

Howell, S. B. 1989, *PASP*, 101, 616

Hubble, E. 1929, *Proceedings of the National Academy of Science*, 15, 168

Iben, Jr., I., & Tutukov, A. V. 1984, *ApJS*, 54, 335

Ji, S., Fisher, R. T., García-Berro, E., et al. 2013, *ApJ*, 773, 136

Johnson, D. R. H., & Soderblom, D. R. 1987, *AJ*, 93, 864

Jordan, S. 2014, *ArXiv e-prints*, arXiv:1411.5206

Jura, M., & Young, E. D. 2014, *Annual Review of Earth and Planetary Sciences*, 42, 45

Just, A., & Jahreiß, H. 2010, *MNRAS*, 402, 461

Kasen, D., & Nugent, P. E. 2013, *Annual Review of Nuclear and Particle Science*, 63, 153

Katz, B., & Dong, S. 2012, *ArXiv e-prints*, arXiv:1211.4584

Katz, B., Dong, S., & Kushnir, D. 2014, *ArXiv e-prints*, arXiv:1402.7083

Kawaler, S. D. 2014, *ArXiv e-prints*, arXiv:1410.6934

Kawaler, S. D., Novikov, I., & Srinivasan, G., eds. 1997, *Stellar remnants*

Kilic, M., Hermes, J. J., Gianninas, A., et al. 2014, MNRAS, 438, L26

Kleinman, S. J., Kepler, S. O., Koester, D., et al. 2013, ApJS, 204, 5

Koester, D., & Knist, S. 2006, A&A, 454, 951

Koester, D., Provencal, J., & Gänsicke, B. T. 2014, A&A, 568, A118

Koester, D., Schulz, H., & Weidemann, V. 1979, A&A, 76, 262

Krzesinski, J., Kleinman, S. J., Nitta, A., et al. 2009, A&A, 508, 339

Külebi, B., Ekşi, K. Y., Lorén-Aguilar, P., Isern, J., & García-Berro, E. 2013, MNRAS, 431, 2778

Kushnir, D., Katz, B., Dong, S., Livne, E., & Fernández, R. 2013, ApJ, 778, L37

Landsman, W. B. 1993, in *Astronomical Society of the Pacific Conference Series*, Vol. 52, *Astronomical Data Analysis Software and Systems II*, ed. R. J. Hanisch, R. J. V. Brissenden, & J. Barnes, 246

Lawrie, K. A., Burleigh, M. R., Dufour, P., & Hodgkin, S. T. 2013, MNRAS, 433, 1599

Lemaître, G. 1933, *Annales de la Société Scientifique de Bruxelles*, 53, 51

Lemaître, G. A., & MacCallum, M. A. H. 1997, *General Relativity and Gravitation*, 29, 641

Lenz, P., & Breger, M. 2005, *Communications in Asteroseismology*, 146, 53

Li, W., Chornock, R., Leaman, J., et al. 2011, MNRAS, 412, 1473

Liebert, J., Bergeron, P., & Holberg, J. B. 2005, ApJS, 156, 47

Liebert, J., Harris, H. C., Dahn, C. C., et al. 2003, AJ, 126, 2521

Livio, M., Pringle, J. E., & Wood, K. 2005, ApJ, 632, L37

Lomb, N. R. 1976, Ap&SS, 39, 447

Maoz, D., Badenes, C., & Bickerton, S. J. 2012, ApJ, 751, 143

Maoz, D., Mannucci, F., & Nelemans, G. 2014, ARA&A, 52, 107

Markwardt, C. B. 2009, in *Astronomical Society of the Pacific Conference Series*, Vol. 411, *Astronomical Society of the Pacific Conference Series*, ed. D. A. Bohlender, D. Durand, & P. Dowler, 251

McMillan, P. J. 2011, MNRAS, 414, 2446

Mestel, L. 1952, MNRAS, 112, 583

Montgomery, M. H., Williams, K. A., Winget, D. E., et al. 2008, ApJ, 678, L51

- Mullally, F., Winget, D. E., De Gennaro, S., et al. 2008, *ApJ*, 676, 573
- Munn, J. A., Monet, D. G., Levine, S. E., et al. 2004, *AJ*, 127, 3034
- Naoz, S., & Fabrycky, D. C. 2014, *ApJ*, 793, 137
- Nomoto, K., Saio, H., Kato, M., & Hachisu, I. 2007, *ApJ*, 663, 1269
- Pakmor, R., Kromer, M., Taubenberger, S., & Springel, V. 2013, *ApJ*, 770, L8
- Paxton, B., Cantiello, M., Arras, P., et al. 2013, *ApJS*, 208, 4
- Pelletier, C., Fontaine, G., Wesemael, F., Michaud, G., & Wegner, G. 1986, *ApJ*, 307, 242
- Perlmutter, S., Aldering, G., Goldhaber, G., et al. 1999, *ApJ*, 517, 565
- Phillips, M. M. 1993, *ApJ*, 413, L105
- Piro, A. L., Thompson, T. A., & Kochanek, C. S. 2014, *MNRAS*, 438, 3456
- Press, W. H., Teukolsky, S. A., Vetterling, W. T., & Flannery, B. P. 1992, *Numerical recipes in C. The art of scientific computing*, ed. Press, W. H., Teukolsky, S. A., Vetterling, W. T., & Flannery, B. P.
- Raskin, C., Scannapieco, E., Fryer, C., Rockefeller, G., & Timmes, F. X. 2012, *ApJ*, 746, 62
- Reichart, D., Nysewander, M., Moran, J., et al. 2005, *Nuovo Cimento C Geophysics Space Physics C*, 28, 767
- Reid, M. J., & Brunthaler, A. 2004, *ApJ*, 616, 872
- Riess, A. G., Filippenko, A. V., Challis, P., et al. 1998, *AJ*, 116, 1009
- Rowell, N. 2013, *MNRAS*, 434, 1549
- Ruiter, A. J., Belczynski, K., & Fryer, C. 2009, *ApJ*, 699, 2026
- Scargle, J. D. 1982, *ApJ*, 263, 835
- Schmidt, M. 1968, *ApJ*, 151, 393
- Schwarz, H. E., Ashe, M. C., Boccas, M., et al. 2004, in *Presented at the Society of Photo-Optical Instrumentation Engineers (SPIE) Conference, Vol. 5492, Society of Photo-Optical Instrumentation Engineers (SPIE) Conference Series*, ed. A. F. M. Moorwood & M. Iye, 564–573
- Schwarzenberg-Czerny, A. 1998, *MNRAS*, 301, 831
- Schwarzschild, M. 1958, *Structure and evolution of the stars*.
- Shapiro, S. L., & Teukolsky, S. A. 1983, *Black holes, white dwarfs, and neutron stars: The physics of compact objects*

- Shapley, H. 1914, *ApJ*, 40, 448
- Sion, E. M., Bond, H. E., Lindler, D., et al. 2012, *ApJ*, 751, 66
- Sion, E. M., Fritz, M. L., McMullin, J. P., & Lallo, M. D. 1988, *AJ*, 96, 251
- Sion, E. M., Holberg, J. B., Oswalt, T. D., et al. 2014, *AJ*, 147, 129
- Sokoloski, J. L., Luna, G. J. M., Mukai, K., & Kenyon, S. J. 2006, *Nature*, 442, 276
- Solheim, J.-E. 2010, *PASP*, 122, 1133
- Starrfield, S., Iliadis, C., Timmes, F. X., et al. 2012a, *Bulletin of the Astronomical Society of India*, 40, 419
- Starrfield, S., Timmes, F. X., Iliadis, C., et al. 2012b, *Baltic Astronomy*, 21, 76
- Starrfield, S., Truran, J. W., Sparks, W. M., & Kutter, G. S. 1972, *ApJ*, 176, 169
- Stetson, P. B. 1987, *PASP*, 99, 191
- Taylor, J. 1997, *Introduction to Error Analysis, the Study of Uncertainties in Physical Measurements*, 2nd Edition, ed. Taylor, J. (University Science Books)
- Thompson, S. E., & Mullally, F. 2009, *Journal of Physics Conference Series*, 172, 012081
- Tremblay, P.-E., Bergeron, P., & Gianninas, A. 2011, *ApJ*, 730, 128
- Tremblay, P.-E., Kalirai, J. S., Soderblom, D. R., Cignoni, M., & Cummings, J. 2014, *ApJ*, 791, 92
- van Kerkwijk, M. H. 2013, *Royal Society of London Philosophical Transactions Series A*, 371, 20236
- van Kerkwijk, M. H., Chang, P., & Justham, S. 2010, *ApJ*, 722, L157
- van Kerkwijk, M. H., & Kulkarni, S. R. 1995, *ApJ*, 454, L141
- Vuille, F. 2000, *MNRAS*, 313, 179
- Vuille, F., & Brassard, P. 2000, *MNRAS*, 313, 185
- Walker, A. R., Boccas, M., Bonati, M., et al. 2003, in *Presented at the Society of Photo-Optical Instrumentation Engineers (SPIE) Conference*, Vol. 4841, *Society of Photo-Optical Instrumentation Engineers (SPIE) Conference Series*, ed. M. Iye & A. F. M. Moorwood, 286–294
- Warner, B. 2003, *Cataclysmic Variable Stars* (Cambridge University Press), doi:10.1017/CB09780511586491
- Webbink, R. F. 1984, *ApJ*, 277, 355

- Wegg, C., & Phinney, E. S. 2012, MNRAS, 426, 427
- Weidemann, V. 2005, in Astronomical Society of the Pacific Conference Series, Vol. 334, 14th European Workshop on White Dwarfs, ed. D. Koester & S. Moehler, 15
- Weidemann, V., & Koester, D. 1984, A&A, 132, 195
- Werner, K., Rauch, T., Barstow, M. A., & Kruk, J. W. 2004, A&A, 421, 1169
- Whelan, J., & Iben, Jr., I. 1973, ApJ, 186, 1007
- Williams, K. A., Bolte, M., & Koester, D. 2009, ApJ, 693, 355
- Williams, K. A., Liebert, J., Bolte, M., & Hanson, R. B. 2006, ApJ, 643, L127
- Williams, K. A., Montgomery, M. H., & Winget, D. E. 2012, in American Astronomical Society Meeting Abstracts, Vol. 219, American Astronomical Society Meeting Abstracts #219, #250.03
- Williams, K. A., Winget, D. E., Montgomery, M. H., et al. 2013, ApJ, 769, 123
- Winget, D. E., Hansen, C. J., Liebert, J., et al. 1987, ApJ, 315, L77
- Winget, D. E., & Kepler, S. O. 2008, ARA&A, 46, 157
- Yaron, O., Prialnik, D., Shara, M. M., & Kovetz, A. 2005, ApJ, 623, 398
- Zhu, C. 2014, ArXiv e-prints, arXiv:1410.4580
- Zhu, C., Chang, P., van Kerkwijk, M. H., & Wadsley, J. 2013, ApJ, 767, 164
- Zorotovic, M., Schreiber, M. R., & Gänsicke, B. T. 2011, A&A, 536, A42